Magnetic and Thermal Properties of Dysprosium Aluminum Garnet. I. Experimental Results for the Two-Sublattice Phases*

D. P. Landau,† B. E. Keen,‡ B. Schneider,§ and W. P. Wolf
Becton Center, Yale University, New Haven, Connecticut 06520
(Received 12 October 1970)

In a magnetic field along a ⟨111⟩ axis, dysprosium aluminum garnet (DAG) closely resembles a two-sublattice Ising antiferromagnet, and it undergoes a transition to the paramagnetic state without spin flopping. To investigate the nature of this transition, high-resolution measurements have been made of the isothermal magnetization and the specific heat C_H as a function of temperature from 1.1 to 4.2 °K in magnetic fields up to 14 kOe. A number of additional measurements have also been made down to 0.5 °K and between 4.2 and 8 °K. Small lattice contributions to the specific heat were estimated from separate measurements on yttrium and lutetium aluminum garnets. The magnetic measurements were made on a small spherical crystal and the thermal measurements were made on a large ellipsoidal single crystal with a demagnetizing factor $N=5.35$. The two sets of data are shown to be consistent if the expected shape dependence is taken into account, and the principal results are converted to correspond to the ideal case of $N=0$. The analysis indicates that the transition is of first order below 1.66 °K, with a region of coexistence between the antiferromagnetic and paramagnetic phases, depending on sample shape. The corresponding latent heat was measured directly and compared with the predictions of the magnetic Clausius-Clapeyron equation. Between 1.66 and 2.53 °K the transition is higher than first order and unusual in form, with fairly sharp but finite maxima in the specific heat and only mild inflections in the magnetic isotherms. A complete phase diagram was constructed, and the principal thermodynamic functions (internal energy, entropy, and enthalpy) were derived. Possible applications of DAG to low-temperature heat engines are discussed briefly. The phase diagram corresponding to $N=0$ shows a general similarity to the phase diagram for He^3-He^4 mixtures, but the analogy is complicated by long-range dipolar forces, known to be significant in the present case.

I. INTRODUCTION

The properties of dysprosium aluminum garnet (DAG) have been studied extensively over the past few years. Low-field susceptibility,[1] magnetization,[2-5] specific-heat,[6-11] magnetic-resonance,[1,12-15] x-ray and neutron scattering,[16-22] optical-absorption,[23-37] Mössbauer-spectroscopy,[38] thermal-expansion,[39] and torque[40] measurements have all indicated that DAG is an unusually interesting system which combines a basic simplicity with some structural complexity to produce a variety of novel properties.

At low temperatures a strong and highly anisotropic crystal field constrains the moment of each Dy^{3+} ion to point along one of the three cubic crystal axes, and when the material undergoes a magnetic phase transition near 2.5 °K, it orders as a six-sublattice antiferromagnet. In the presence of a magnetic field along the [111] axis[41] these sublattices become equivalent in threes, $(+x,+y,+z)$ and $(-x,-y,-z)$, and we may treat the system as a simple two-sublattice antiferromagnet.

As the strength of the field is increased there is a phase transition in which the spins in the minus sublattice reverse their directions and the system becomes paramagnetic with a net moment along [111]. The transition is unusual for an antiferromagnet in that it proceeds apparently without any intermediate "spin-flop" state. In fact, the system may be described with considerable accuracy in terms of a simple two-sublattice Ising-model antiferromagnet whose effective spins can only point along $\pm\vec{H}$.[21] The detailed discussion of the validity of this description will be deferred to a later paper, which we shall henceforth refer to as II.

For the present we shall regard the phase transition from a thermodynamic point of view and we shall present a series of magnetic and thermal measurements which give a macroscopic description of the transition as a function of field and temperature. We shall show that the very nature of the phase change varies with temperature in a rather unusual manner, being of first order at low temperatures but higher than second order just below the Néel point.

The behavior is complicated by shape-dependent effects arising from long-range magnetic dipole interactions common to *all* magnetic systems, but here especially noticeable because of the relatively high magnetic density. By using accurately shaped spherical and ellipsoidal single crystals it is possible to relate these effects to a spatially homogeneous demagnetizing field and to express all the results in terms of more intrinsic functions of the *internal* magnetic field and temperature. In the

case of the thermal measurements this requires an analysis which combines both thermal and magnetic data[42] and it is necessary to check for the internal consistency of different measurements, especially if these are made on different samples. Fortunately such checks can readily be made by comparing various thermodynamic derivatives, and while it is sometimes difficult to achieve high accuracy, a generally satisfactory situation can be established.

In addition to providing information about the phase transition, magnetothermal measurements can also be used to give quantitative estimates of various parameters which characterize the behavior of systems more generally. These parameters are of two kinds: coefficients of macroscopic properties in regions where the theory is simply related to the measurements, and terms in a microscopic Hamiltonian describing individual spins and their interactions. Examples of the first kind are the Curie and Curie-Weiss constants, critical fields at $T = 0\,^{\circ}\mathrm{K}$, and the parameters characterizing the spin-wave excitation spectrum. The second kind includes the effective g factor and the coefficients of the magnetic and exchange interactions between different neighboring spins in the crystal lattice.

It is convenient to discuss these two types of analyses separately and we shall do this in two further papers in the present series (II and IV). In another paper (III) we plan to present results and an analysis of measurements similar to those given in the present paper and II, but for field in directions other than [111]. The simple two-sublattice model does not apply in that case and one has to consider more complex multisublattice situations. However, even then one can extract some macroscopic parameters which can be related to the microscopic terms in the complete Hamiltonian and this will be done in IV, together with the results for the [111] fields.

Only then shall we be in a position to attempt a detailed comparison between the predictions of various statistical approximations and the observed phase transitions, and such comparisons may be considered in later papers. However, the main purpose of the present series is to present a fairly detailed description of the thermodynamic behavior of DAG and to derive an accurate spin Hamiltonian for the system. As we shall see, this turns out to be very similar to that of the commonly considered Ising models, but with a few important differences. In particular there are significant interactions between neighbors other than the nearest neighbors, and the competition between these interactions is probably responsible for the unusual phase transition which is observed. There are only primitive theories for such cases, and it is our hope that the present results will lead to further refinements of the theory.

The present paper deals with three different kinds of measurements: high-resolution isothermal magnetization, specific heats at constant external field, and magnetocaloric measurements in varying fields. The experimental methods are described in Sec. II and the results are discussed in Secs. III and IV. Related thermodynamic functions (internal energy, entropy, and enthalpy) are derived from the experimental data in Sec. V and there is a brief discussion of possible applications of DAG to magnetic heat engines. The shape dependence of the thermodynamic functions is considered in Sec. VI, and curves for the specific heat and entropy at constant *internal* field are derived. The conclusions are summarized in Sec. VII. An appendix contains a brief description of some specific-heat measurements on yttrium and lutetium aluminum garnets (YAG and LuAG) and an estimate of the lattice specific heat of DAG.

Preliminary accounts of some of this work have been published previously in Refs. 7 and 9–11.

II. EXPERIMENTAL

A. Sample Preparation

For the magnetization measurements a spherical sample was ground from a single crystal which had been grown by the standard flux method.[43] The weight of the sample was 44.8 mg and its diameter was 2.40 ± 0.02 mm. The corresponding demagnetizing factor is 4.19 ± 0.05. The sample was aligned by x-ray Laue back reflection and mounted with its $(1\bar{1}0)$ plane horizontal. The [111] axis[41] was located *in situ* by measuring the angular variation of the magnetization in a large field and using the known anisotropy.[3] The final accuracy of alignment with respect to the magnetic field was probably within about 2°, but for the present series of measurements this was not very critical.

For the thermal measurements four large crystals (about 35 g each) were obtained from the Linde division of Union Carbide. These crystals were made by the Czochralski technique of pulling from the melt.[44] All four were roughly cylindrical in shape, about 1.5 cm in diam and about 3 cm long. Three of them were used only for zero-field measurements and these were left as grown with only the ends ground flat for mounting, but the fourth crystal was accurately shaped into an ellipsoid of revolution 33 mm long and 14 mm in diam, with its axis of symmetry parallel to one of the ⟨110⟩ axes. The sample was aligned and mounted similarly to the sphere, so that the magnetic field could also be swept over all directions in the $(1\bar{1}0)$ plane. The demagnetizing factor was $N = 5.35 \pm 0.05$ for all directions in this plane, the small uncertainty in N reflecting the precision with which the crystal could be machined. The [111] axis was in this case iden-

tified using the angular dependence of the magnetocaloric effect[8]; the accuracy of alignment was again about 2°.

Spectroscopic analysis of chips taken from the ellipsoidal sample showed that the major impurity was 100–1000 ppm lanthanum with only faint traces of the other rare earths. No analyses were made on the other samples but it is likely that the impurity contents were similar, except for the flux-grown sample which may have contained some additional lead and platinum, and possibly a small amount of Fe^{3+}. None of these impurities would be expected to affect the properties of DAG on the scale of the present measurements.

A more serious concern is the possibility that the crystals may not have been perfectly stoichiometric with respect to the Dy : Al ratio, especially for the Czochralski crystals which are grown at very high temperatures (~ 2000 °C). This ratio is very difficult to determine directly, but as a check one can measure the bulk densities and the x-ray lattice constants. Gravimetric measurements of the large crystals indicated densities ranging from 6.191 ± 0.001 to 6.204 ± 0.001 g/cm^3, while lattice constants varied from 12.0408 ± 0.0003 to 12.056 ± 0.001 Å. The literature value for DAG is 12.05 Å.[16] There was no obvious relationship between the two kinds of measurements but the variations are all quite small and it seems unlikely that there are any serious deviations from stoichiometry. However, the possibility of small variations remains, and this seems to be the most likely cause of the spread in Néel temperatures (~ 0.023 °K) found for different samples (see Sec. IV). Such differences become troublesome if magnetic and thermal measurements made on different samples are combined in a thermodynamic analysis. Fortunately in our case, the small sphere and the ellipsoid had almost identical Néel points and no correction had to be applied.

B. Magnetization Measurements

High-resolution magnetization measurements were made with a Foner-type vibration magnetometer,[45] operating at 34 Hz. In order to reduce stray pickup astatically wound coils were used for both the sample and reference signals and a PAR HR-8 lock-in detector was used to find the null point. The reference signal was varied by adjusting a dc current through a small coil vibrating on the sample rod near the reference pickup coils near the top of the apparatus. This method has the advantage that the dc current can be measured very accurately using an integrating digital voltmeter, and we used a Dymec 2401C. The smallest change in the sample magnetic moment which could be detected was about 2×10^{-4} emu, corresponding to one part in 2×10^4 of the saturation moment of our 44.8-mg DAG sample.

The magnetometer was originally calibrated with a sphere of 99.999% pure nickel, using $M_{sat} = 54.39$ emu/g at 20 °C,[46] and later against the susceptibility of manganous ammonium sulphate (MAS) taking[47] the molar Curie constant to be 4.375 (°K)$^{-1}$. These two methods disagreed by about 1% and a mean value was finally used for converting all the experimental results into absolute units. However, since the completion of this part of the work, it has been found that the old literature value for the M_{sat} of Ni was incorrect and taking the new value[48] we get a result which is consistent with that for MAS and about 0.5% higher than the mean value which was used. All the results given in this paper should therefore be increased by about 0.5%, but we have not done this as this is comparable with other possible systematic errors and the change would not affect any of our conclusions significantly. Moreover, we shall see in Sec. III that the calibration constant actually used may in fact have been even closer to the correct value than 0.5% and we therefore choose to absorb all the uncertainties in an overall calibration error of ± 0.5%.

In order to check for possible errors due to small changes in the position of the sample relative to the pickup coils, a standardizing measurement at 14 kOe and 4.2 °K was made after each helium fill. In no case did these measurements vary by more than 0.5%, and we can conclude that the over-all accuracy of the magnetization measurements was better than ± 1%.

The magnetic field was provided by a 12-in. PEM electromagnet and in most cases it was measured with a Rawson Gaussmeter which had been calibrated with nuclear magnetic resonance. The reproducibility of these measurements was better than 0.1%. However, for some of the high-resolution measurements in the vicinity of the phase transition considerably more accurate field values were required, and for these we used the NMR gaussmeter directly. The accuracy of these measurements was limited by field inhomogeneities at the site of the gaussmeter probe to about ± 0.3 Oe.

In order to avoid magnetocaloric effects, which are quite large in materials like DAG, measurements were taken point by point, repeating each reading until a consistent value was obtained. In practice it was possible to take measurements in steps as small as 25 Oe with sufficient accuracy to yield values of $\Delta M/\Delta H$ consistent to 1%.

Temperatures were measured from the vapor pressure of the liquid helium surrounding the sample space, which contained about 200 μ of helium exchange gas to establish thermal contact. Coarse control of the bath temperature was achieved with a Walker-type pressure regulator[49] and fine adjustments were made with a heater at the bottom of the

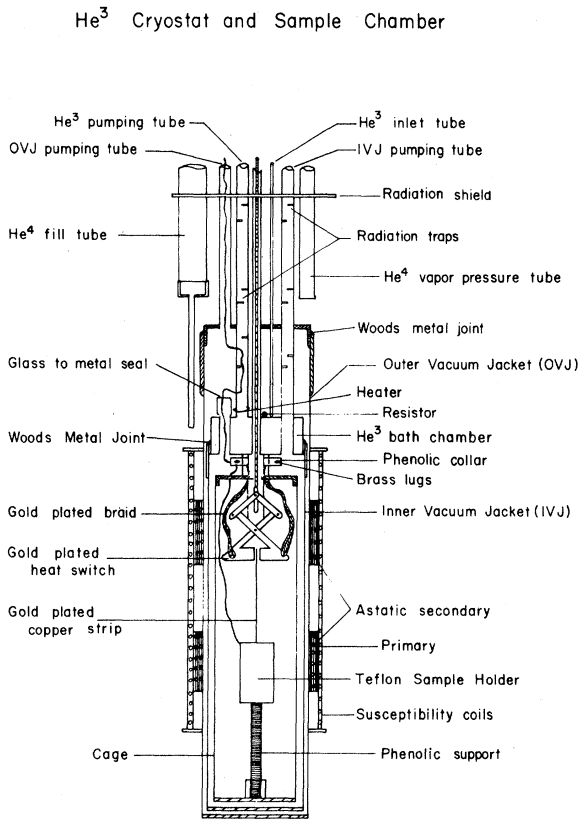

FIG. 1. He^3 cryostat used for measurements of specific heat and for adiabatic and isothermal field sweeps.

Dewar, using a carbon resistance thermometer close to the sample as a sensor. The heater also served as a stirrer above the λ point where hydrostatic head corrections can be as big as 20 m °K. The absolute accuracy of the temperature measurements was generally between ±5 and ±10 m °K, except for a small region very close to the λ point where it may have been somewhat larger. The relative temperature stability, however, could be maintained considerably better than this, and the error due to magnetoresistance in the carbon thermometer did not exceed 2 m °K over the field range covered by the phase transition. The absolute accuracy was confirmed by the calibration measurement on MAS, while the temperature stability could be checked from the DAG phase transition itself.

C. Specific-Heat Measurements

1. *Calorimeter and Experimental Procedure*

Two cryostats were used for the thermal measurements. A simple He^4 cryostat was used for the initial experiments, and this was later replaced by an improved apparatus which could also be used with He^3 for reaching lower temperatures. The general characteristics of the first cryostat were similar to those of the second and we shall not describe it separately.

Figure 1 shows the low-temperature section of the He^3 cryostat which was of the standard "single-shot" type. One important feature for specific-heat measurements is the efficiency of a heat switch, which avoids the use of exchange gas.[50] Our switch was made of copper as shown, with the mandibles gold plated to improve thermal contact to the similarly gold-plated copper strip attached to the sample. With the switch closed the heat flow across the contact was of the order of 500 erg/sec at 2.5 °K with the sample only 0.2 °K higher in temperature than the inner vacuum jacket (IVJ). With the jacket at 1.1 °K and the sample initially at 4.2 °K the heat flow was better than 2000 erg/sec. For the 20-g DAG sample used, this implied cooling times of the order of 2 h for 4.2 to 1.2 °K. The heat developed on opening the switch varied from 1000 erg to as little as 100 erg, depending on how slowly the switch was opened and how well the strip leading to the sample was centered. (Generally, vibration of the sample caused by the operation of the switch was a greater source of heat input than the heat actually developed while opening the switch.)

Another important feature of our apparatus was the method of supporting the sample. For zero-field measurements this presents no special problem, and we used a simple brass holder attached to a stainless-steel cage by cotton threads. However, for measurements in large fields a much more rigid support is required. Typical torques on our DAG sample were 10^6 dyn cm and after a number of catastrophic experiments we finally used a Phenolic tube 6-mm o.d. and 4-mm i.d. to support a Teflon container enclosing the sample, and even this broke after some time! The heat capacities of both holders were estimated from separate experiments and subtracted from the measured totals. That of the brass holder was found to be very small and essentially negligible compared to that of DAG, but the Teflon holder entailed a much larger correction equivalent to $C/R \sim 1.7\times10^{-3}T^3$ (T in °K) for our sample.

Another disadvantage of using the Phenolic and Teflon support was a rather high heat influx from the surroundings, and in practice this limited the temperature resolution between successive heat-capacity measurements to about 1 m °K. In zero field, on the other hand, it was possible to measure temperature changes to 1 μ °K and to obtain specific-heat measurements every 50 μ °K.

To cut down the uncertainty from stray heat influx, the temperature of the sample environment was carefully controlled. The temperature of the He^3 in the cryostat was controlled in the usual way by adjusting the pumping rate, but in addition an electrical heater and thermometer were used to stabilize the temperature. The thermometer was

a $\frac{1}{2}$-W 470-Ω-type 1002 Speer carbon resistor wrapped with a thin copper strip, the other end of which was attached to one of the bushings in the top of the He^3 bath chamber (see Fig. 1). The heater was a 1-m length of 0.002-in. Evanohm wire wrapped bifilarly around another bushing. The thermometer formed one arm of a Wheatstone bridge and a PAR model JB-5 lock-in detector was used as a null detector, with the output being fed back into the heater. In this way the temperature of the inner vacuum jacket could be stabilized to within 10 m °K over periods of 2 h.

Another precaution to reduce stray heat influx was to ensure that the various leads going to the sample were thermally anchored to the temperature of the He^4 bath and to the IVJ. The arrangement for this is indicated in Fig. 1.

Heat-capacity measurements were made by the usual heat pulse method in which electrical power is supplied to a heater for a short period and the change of temperature is determined from drift rates before and after the heating. The heater consisted of about 150 cm of 0.002-in. (0.05-mm) diam insulated Evanohm wire wound noninductively on the sample or on the sample holder, using GE 7031 varnish to ensure thermal contact. The heater resistance was typically 1100 to 1200 Ω and the resistance of the current carrying leads (manganin) was about 60 Ω. To allow for the heat developed in the leads and conducted to the sample, the heater power was measured using potential leads attached to the current carrying leads halfway between the last heat sink and the sample.[51]

The current through the heater was measured using a Dymec 2401C digital voltmeter with a Dymec 2411A preamplifier and a standard 1000-Ω resistor. To prevent variations in the current, a dummy load was used whenever the current was not passing through the sample heater, and its resistance adjusted to be exactly equal (±0.1%) to that of the heater. The current could therefore be measured at leisure while the sample was not being heated. The voltage across the sample heater and the length of the heating pulse were measured using the same digital voltmeter, operating in the integrating mode to determine $\int V\,dt$ directly. Because the current was essentially constant, this integral multiplied by the current gives an accurate measure of the total energy supplied during the heat pulse. Typical heater powers were 10^{-5} to 4×10^{-4} W and the length of the pulses ranged from 10 to 100 sec. The time required for the reestablishment of a constant drift rate after the heating pulse varied from 25 sec to 5 min, depending on the amount of energy added and the thermal diffusivity. Measurements of the drift were generally continued for about four times this period. In almost all cases the change in temperature due to the heat pulse was more than ten times the drift during the reestablishment of equilibrium, and it was generally possible to determine the temperature rise due to the heat input to better than ±0.5%.

Whenever the specific heat is not linear in temperature, a correction must be made for curvature in calculating results from finite heating steps. The method we adopted was to calculate the average specific heat and to correct the temperature to a suitably weighted mean using measurements from adjacent points.

For measurements in external magnetic fields we used the same electromagnet as for the magnetometer. Due to the larger Dewar size it was not possible to use NMR to measure the fields during actual runs, but by careful calibration of the rotating-coil gaussmeter, field measurements accurate to ±0.1% could still be made.

2. *Temperature Measurement and Calibration*

To measure the temperature of the sample, $\frac{1}{2}$-W Allen Bradley and Speer carbon resistors (nominal resistances 68 and 470 Ω) were used. The former were best for the range 1.2–4.2 °K and the latter between 0.5 and 1.5 °K. No special treatment such as grinding off the outer surface was given to the resistors, but care was taken to ensure good thermal equilibrium by using "coil foil"[52] and GE varnish to attach the thermometers. Resistances were measured with a Wheatstone bridge using a PAR model HR-8 lock-in detector, both as a source and as null detector. A Triad G-10 "Geoformer" was used to isolate the source output from the detector and a 0.001-μF mica capacitor was put in parallel with the thermometer to eliminate rf heating from local radio and TV stations.[53] The contribution of lead resistances was eliminated by using dummy leads and a 1:1 ratio on the Wheatstone bridge. The bridge was operated at 33 or 94 Hz with power inputs ranging from 10^{-7} to 10^{-10} W. For a resistance of the order of 16 kΩ, the maximum sensitivity was ±0.02 Ω, corresponding to ±1 μ °K at 2.5 °K.

The thermometers were calibrated over three different temperature ranges, a new calibration being taken each time the thermometer was allowed to warm up or a different magnetic field was used, although the changes were always quite small. Between 4.2 and 1.1 °K the calibration was against the vapor pressure of He^4, care being taken to guard against hydrostatic head effects as in the magnetometer experiments (see Sec. II B). Between 1.5 and 0.37 °K the vapor pressure of He^3 was used.[54] A significant correction had to be applied for thermomolecular pressure,[55] even though we used an unusually wide (6-mm) vapor pressure tube.

Above 4.2 °K the calibration was against the susceptibility of manganous ammonium sulphate, which was measured with a mutual inductance coil (see

Fig. 1), and the usual ac Hartshorn bridge.[47] For a material such as MAS the mutual inductance is given by an expression of the form

$$M = \frac{\lambda}{T-\theta} + M_0 , \tag{1}$$

where λ is proportional to the Curie constant and θ can be estimated from previous measurements[47] and a knowledge of the shape of the sample. The term M_0 represents the inductance in the absence of the sample and this may vary with the temperature of the cryostat. To eliminate this effect, the susceptibility calibration was made keeping the cryostat fixed at 1.1 °K and varying only the temperature of the MAS sample and carbon thermometer by means of a separate heater. In range 1.1–4.2 °K the temperature of the sample could be inferred from the prior calibration of the resistor against the vapor pressure of He^4 and the constants λ and M_0 in Eq. (1) could thus be determined. Above 4.2 °K, M could then be used to indicate the temperature for the further calibration of the resistor. The accuracy of this method is not very high and we estimate an error of ± 0.05 °K at 8 °K but this was adequate for our measurements in this range.

As a check on this part of the calibration an additional fixed point measurement was made of the superconducting transition in lead. This could be determined to an accuracy of ± 0.005 °K from the jump in the susceptibility of a small cylindrical sample whose transition had previously been found to be 7.193 °K.[56,57] The agreement was within our estimated uncertainty.

Each calibration run was fitted to an expression of the form

$$\frac{1}{T} = \sum_{n=-1}^{4} a_n (\ln R)^n \tag{2}$$

using the Yale 7040-7094 DCS computer. To avoid truncation and rounding difficulties, particularly when processing the high-resolution specific-heat data, all programs were written to use 16 significant figures. The fitting procedure allowed the rejection of points which were clearly in error, and it was also possible to include terms with $n > 4$ in Eq. (2). However, this usually brought no significant improvement in the fit. It is difficult to estimate the over-all accuracy of the calibration procedure but it was almost certainly better than ± 10 m °K over the whole range 4.2–0.4 °K.

D. Magnetocaloric Measurements

Because of the rapid response of both the thermometer and the lock-in detector, it was possible to follow magnetocaloric effects in both adiabatic and isothermal magnetic field sweeps. For this purpose the magnet was controlled with a simple electromechanical sweep generator which provided sweep rates between 10 and 10^4 Oe/min.

The adiabatic sweeps were quite straightforward and two different techniques were used to follow the temperatures. In the first the resistance bridge and the Rawson gaussmeter were balanced simultaneously and corresponding field-temperature values determined. In the second, the lock-in detector and gaussmeter were used off balance and their output recorded directly on an X-Y recorder. The field sweep was quite linear and the calibration of the field axis presented no problem. For the calibration of the resistance (temperature) axis a variable dummy load was connected in series with the thermometer, so that any resistance value could be simulated and compared with points on the sweep tracings. In this way it was possible to measure even large changes in resistance corresponding to the very appreciable magnetocaloric temperature changes which were sometimes observed. However, for accurate measurements, the null method is probably preferable.

One serious problem with "adiabatic" sweeps is that it is generally very difficult to estimate the amount of stray heat reaching the sample while its temperature is different from that of the cryostat. By measuring the difference between the initial and final temperature in a complete field cycle one can find the total amount of entropy supplied to the sample, but this may be due to either magnetic irreversibilities or to stray heat leaks. In principle it is possible to stop the sweep at some intermediate point and to observe the drift rate of the temperature. By using previously measured values of the specific heat one can then determine the heat influx and attempt an estimate of the effect on the adiabatic curves. In practice this is quite difficult and we have not attempted to find this correction. Indeed we have so far restricted ourselves to drawing only semiquantitative conclusions from the adiabatic field sweeps (see Sec. IV), and for these the corrections are not important. However, the method itself is capable of significant development and we plan to make further measurements of this kind in the future.

The isothermal sweeps were performed by taking the off-balance output from the lock-in (set on as sensitive a range as possible) and feeding it to the specimen heater. The output was also put on an X-t recorder and simultaneously monitored on the digital voltmeter. Field calibration points were taken periodically, and a temperature drift rate was taken at the beginning and end of each trace. By adjusting the initial sample and cryostat temperatures to be nearly equal, these drifts could be made negligibly small. The X scale was calibrated against the digital voltmeter reading of the current through the heater, and this could then be converted into the power required to keep the temperature

constant. This is equal to $T(dS/dt)$, and using the measured variation of H with time this gives $T(\partial S/\partial H)_T$.

Because the reaction time constants of the system were small but finite, oscillations sometimes developed due to the heater and thermometer being out of phase. The problem became more acute at high sweep rates and the maximum useful rate was 100 Oe/sec. Below about 4 Oe/sec the magnetocaloric effect became too small to measure accurately, and a practical compromise was usually of the order of 20 Oe/sec.

The main problem with this method is that it is only possible to sweep in one sense [the one for which $(\partial S/\partial H)_T$ is negative], and it is therefore impossible to check for irreversible heating during the process. In general the amount of energy which has to be supplied by the heater will therefore be less than the true change in $T\Delta S$ and indeed evidence for this was obtained in some of our sweeps at the lowest temperatures. In most cases, however, the irreversible heating seemed to be quite small, and evidence for this was obtained from the comparison of the values of $(\partial S/\partial H)_T$ obtained from the isothermal sweeps with values of $(\partial M/\partial T)_H$ obtained from the magnetization isotherms (see Sec. V B).

E. Accuracy and Internal Consistency

In the preceding sections we have given estimates of the errors which may occur in various specific measurements, and in general these are quite small. However, it should be stressed that a number of the experimental results involve a certain amount of additional data processing, such as numerical differentiation and interpolation, and this may increase the errors significantly. Whenever possible, we have therefore attempted to check for internal consistency and we have indicated estimates of the over-all uncertainties by error bars on selected points. In view of the large amount of data obtained it has not been possible to ensure the very highest accuracy in all the determinations, and the present results should therefore be viewed more as an over-all survey rather than a detailed study of certain features which become apparent as the data unfold. In particular we anticipate that it would now be profitable to perform additional measurements on differently shaped samples in selected regions of the phase diagram, but we must defer this for the present.

III. MAGNETIC MEASUREMENTS: RESULTS AND DISCUSSIONS

A. Magnetic Measurements on the Spherical Sample

Measurements of the isothermal magnetization M were made as a function of the applied field H_0 along the [111] axis for 11 temperatures between 1.14 and 4.23 °K. The results are shown in Fig. 2, and they are in good agreement with earlier work.[2,4] No measurable hysteresis was detected at any temperature. In addition to the points shown in Fig. 2, a large number of closely spaced measurements were made in the vicinity of various inflection points and regions of marked curvature. These are best displayed by plotting the ratio of small differences $\Delta M/\Delta H_0$, which is essentially equal to the derivative $(\partial M/\partial H_0)_T$. Figures 3 and 4 show $(\partial M/\partial H_0)_T$ plotted as a function of H_0 for temperatures above and below T_N. These curves reveal a number of striking features which are, of course, also present in Fig. 2, but which are emphasized by taking the derivative.

We may note in particular an absolutely flat region which is independent of temperature for $T < 1.66$ °K, a series of pronounced peaks which vary with T for $1.66 < T < 2.53$ °K, and a second series of broader peaks which persists even above T_N. We shall discuss these features in some detail in Sec. III C, after we have considered the effect of sample shape on the magnetization.

B. Derivation of Magnetic Properties of an Infinite Needle

The effect of sample shape on the magnetic properties of any homogeneous ellipsoidal sample is completely contained in the equation

$$\vec{H}_i = \vec{H}_0 - \overleftrightarrow{N} \cdot \vec{M} \tag{3}$$

where $\overleftrightarrow{N}$ is the classical demagnetizing factor and $\vec{H}_i$ is the internal magnetic field. For an infinite needle magnetized along its length $\overleftrightarrow{N} \cdot \vec{M} = 0$, and for this one shape $\vec{H}_i = \vec{H}_0$. In all other cases one must solve Eq. (3) and in general this can be quite complex since $\vec{M}$, $\vec{H}_0$, and $\vec{H}_i$ need not point along the same directions. However, if as in the present experiments, the principal axes of the demagnetizing tensor coincide with those of the crystal, and $\vec{H}$ is applied along one of these directions, all three vectors will be parallel, and we can replace Eq. (3) by the corresponding scalar form

$$H_i = H_0 - NM\,, \tag{3'}$$

which gives the magnitude of H_i for any measured pair of values of M and H_0. One can then express M as a function of H_i and obtain a relation independent of the original shape. In some respects this may be regarded as more intrinsic, since being free of demagnetizing effects, it will represent the behavior of a single domain in any situation in which it is energetically favorable for the macroscopic magnetization to divide into small regions which combine to cancel the magnetostatic energy of the surface. We shall see that this happens in our magnetic transition below 1.66 °K.

Using Eq. (3′) and the calculated value of N, we can immediately transform Fig. 2 into the corre-

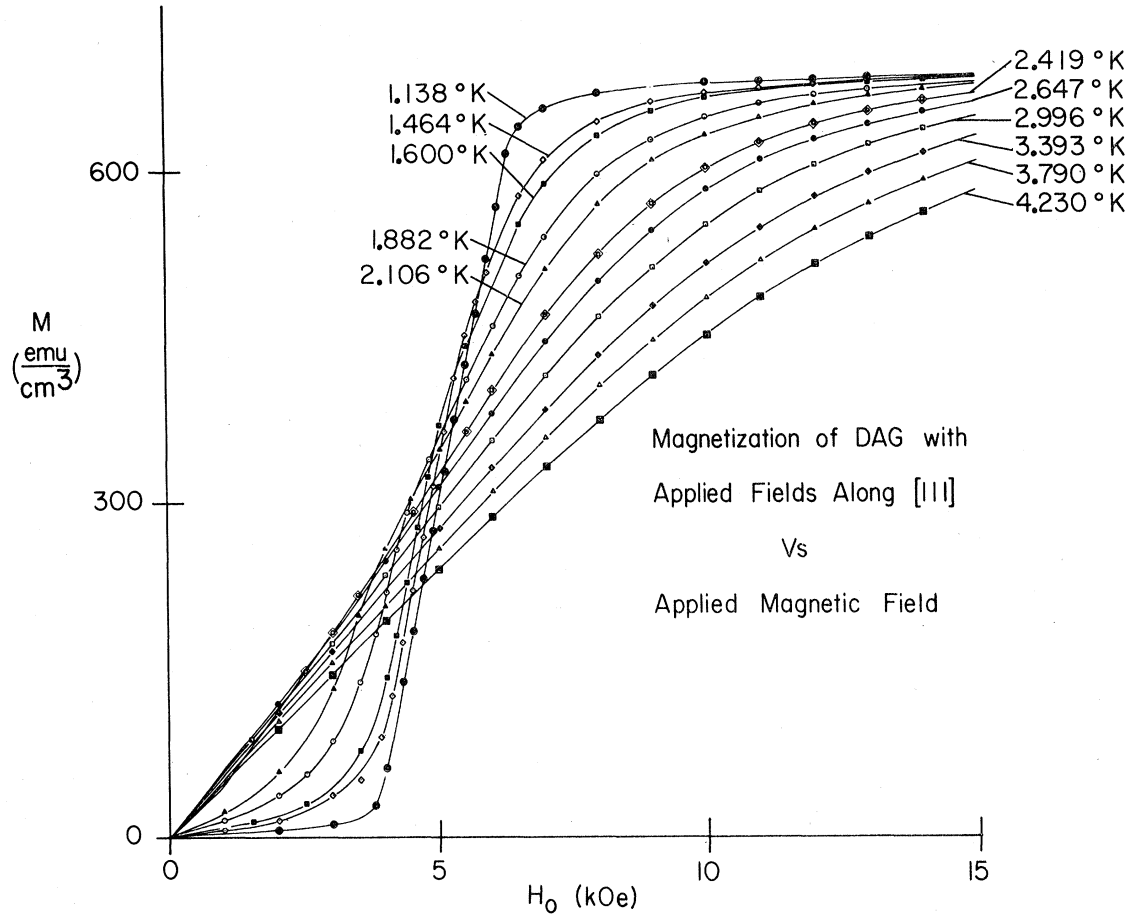

FIG. 2. Isothermal magnetization of a DAG sphere ($N=4.19$) as a function of applied field H_0 along [111] for temperatures between 1.1 and 4.2 °K.

sponding plot of M as a function of H_i for various T. This is shown in Fig. 5. By interpolation we can also obtain M as a function of T for various values of H_i and this is shown in Fig. 6. The corresponding derivatives $(\partial M/\partial H_i)_T$ and $(\partial M/\partial T)H_i$ plotted as functions of both H_i and T are shown in Figs. 7–10. It can be seen that the features previously noted in curves as a function of H_0 are here strongly accented, and in particular the linear region in the M-H_0 isotherms now appears as a vertical discontinuity. This clearly indicates a first-order phase transition.

To demonstrate the accuracy to which the discontinuities are truly vertical, we have plotted in Fig. 11 the isotherm for $T=1.14$ °K on a highly expanded scale. It can be seen that there is a very slight deviation from the vertical but this is readily accounted for by experimental errors. The estimated uncertainties in M and N are each 1% and since ΔM at the transition is about 600 G there is a corresponding uncertainty of 50 Oe in ΔH_i. The actual difference between the two ends of the line is in fact much less than this (~ 10 Oe) and we can conclude that the transition is indeed first order. Conversely, we may use this agreement to provide evidence that our absolute calibration of the magnetometer is correct. Indeed the agreement is better than it should be in view of the slightly incorrect calibration constants which we used (see Sec. II B) and it is tempting to speculate that this phase transition might in fact be used to provide a better absolute standard for calibrating magnetometers than the usual ferromagnet or paramagnet. If N were known to high accuracy, as it could be by careful shaping, only the correct calibration could make the M-H_i curve vertical. However, there is a possibility of small higher-order effects which would have to be eliminated first (see Sec. III C).

The errors in the various derivatives are much larger than those in M or H_0, especially when they are corrected to zero demagnetizing factor, as indicated by the error bars in Figs. 7–10. A check on the internal consistency of the various derivatives can be obtained by evaluating the product

$$\left(\frac{\partial M}{\partial H_i}\right)_T \left(\frac{\partial H_i}{\partial T}\right)_M \left(\frac{\partial T}{\partial M}\right)_{H_i} \tag{4}$$

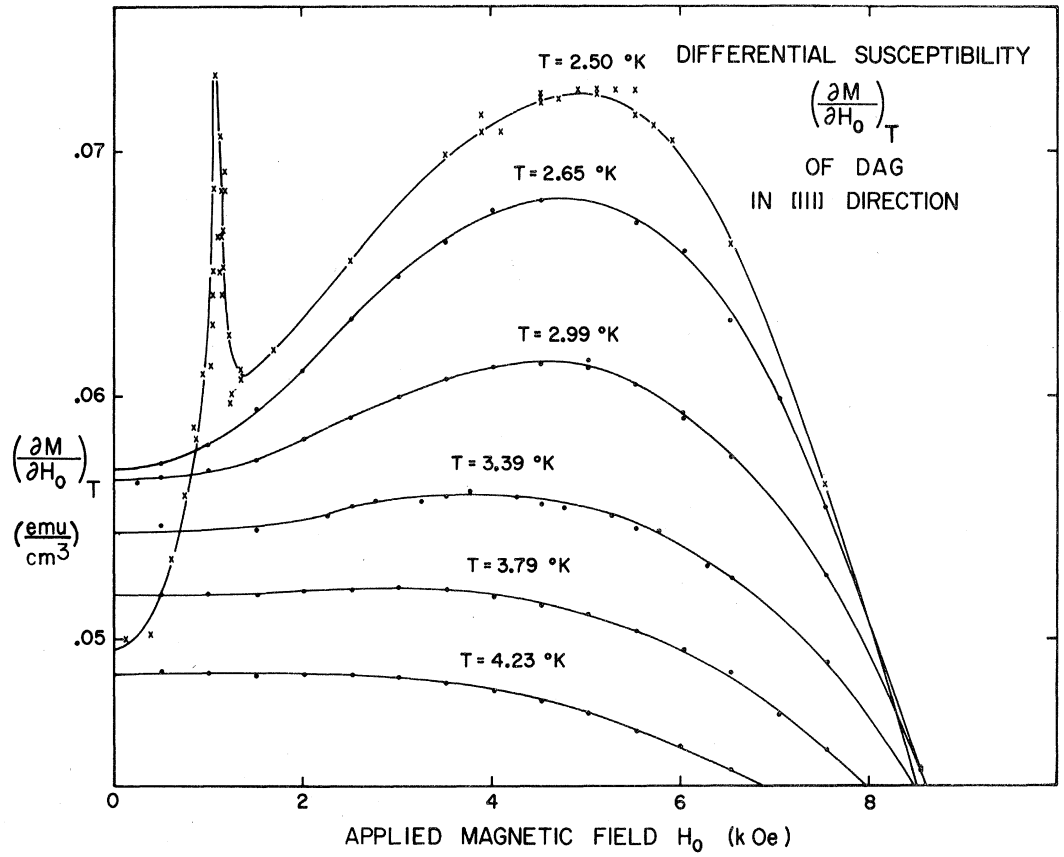

FIG. 3. Differential susceptibility $(\partial M/\partial H_0)_T$ of a DAG sphere as a function of applied field H_0 along [111] for $T \geq 2.50$ °K.

at various points on the M-H_i-T surface. Values ranging from -0.81 to -1.20 were found which may be compared with the ideal value -1, but in all cases the differences were within the estimated experimental uncertainties. As one would expect, the errors were largest in regions near the phase transition or where $(\partial M/\partial T)_{H_i}$ changes sign. Bearing in mind that the products involve products of three numerical differentiations of experimental results, we can regard the over-all consistency as extremely satisfactory.

C. Magnetic Phase Diagrams

The observed magnetic properties clearly indicate three distinct regions of temperature which we can discuss separately: $T_1 < 1.66$ °K $< T_2 < 2.53$ °K $< T_3$.

1. $T < 1.66$ °K

In this range the magnetization versus internal field curve shows a sharp discontinuity indicating a first-order phase change. The values of the magnetization corresponding to the two ends of the discontinuity ($M^{\pm}$) vary with temperature as shown in Fig. 12 and they define two phase boundaries which terminate in a single point ($M_t = 250 \pm 5$ emu/cm^3; $T_t = 1.66 \pm 0.01$ °K). The nature of this type of tricritical point has recently been discussed theoretically by Griffiths,[58] but our present measurements are unfortunately not precise enough to permit any detailed quantitative analysis of the region close to (M_t, T_t). In fact it is doubtful if *any* simple bulk measurements could ever define the M-T phase boundary very precisely near T_t, since $(\partial M/\partial H_i)_T$ seems to diverge on both sides of the transition, so that the actual first-order discontinuity $M^+ - M^-$ becomes very hard to distinguish as it tends to zero.[59]

The internal magnetic field for the phase transition H_i^c, on the other hand, appears to vary with temperature in a well-defined way up to T_t and even beyond (see below), and it defines a simple phase boundary as shown by the broken line in Fig. 13. However, this phase boundary is also not observable experimentally with high precision since its determination from measurements on any finite sample generally involves a sizable demagnetizing correction, which again requires knowledge of the ill-defined critical magnetization.

While the details of the behavior in the immediate

vicinity of the tricritical point are thus hard to determine, the general physical picture at lower temperatures is quite clear. In any finite sample, demagnetizing effects spread the first-order transition over a range of external fields, $H_0^- < H_0 < H_0^+ = H_0^- + N(M^+ - M^-)$ and over this range the paramagnetic and antiferromagnetic phases coexist in varying proportions. For example, the H-T phase diagram corresponding to a sample with $N = 5.35$ is shown in Fig. 13. The experimental points labeled as magnetic measurements were here calculated from the data for the spherical sample, shown in Fig. 2, corrected according to Eq. (3′). The experimental points labeled "thermal measurements" will be discussed below (see Sec. IV).

To understand the effect of applied fields between H_0^+ and H_0^- we need a model of the mixed state consisting of regions of the paramagnetic phase and regions of the antiferromagnetic phase and this has been discussed by Wyatt.[60] Since it is found experimentally that $(\partial M/\partial H_0)$ is accurately constant and equal to $1/N$ over the whole of the coexistence range, we can conclude that the regions must be small compared to the volume of the sample (so that it may be treated as effectively homogeneous), and that energy of the interface between the two phases is also small compared to the total energy. Under these conditions the average magnetization is simply given by

$$M = M_0^- + N(H_0 - H_0^-), \quad H_0^- < H_0 < H_0^+ . \tag{5}$$

No detailed theoretical calculations relating to "domains" in this kind of system exist, but one can make simple order-of-magnitude estimates of the energies involved and these indicate that the domains should indeed be small (~1 μm in diameter) and that the domain-wall contribution to the energy should be negligible.

In view of the close agreement between the experimental value of $(\partial M/\partial H_0)$ and $1/N$ it is tempting to speculate that the correspondence should be exact and that one might even use the measured value as an absolute calibration for the magnetization. However, in addition to the domain-wall energy there is another small contribution to the energy arising from magnetoelastic coupling and this may not be entirely negligible for really accurate comparisons. Unfortunately little is known about magnetostriction in systems such as DAG and one can again only make an order-of-magnitude estimate. One finds[61] that the effect for DAG is in fact quite small (< 0.1% in $\Delta H_0/H_0$) as one might expect from the relatively weak magnetic interactions and high mechanical stiffness. However, in other metamagnetic mater-

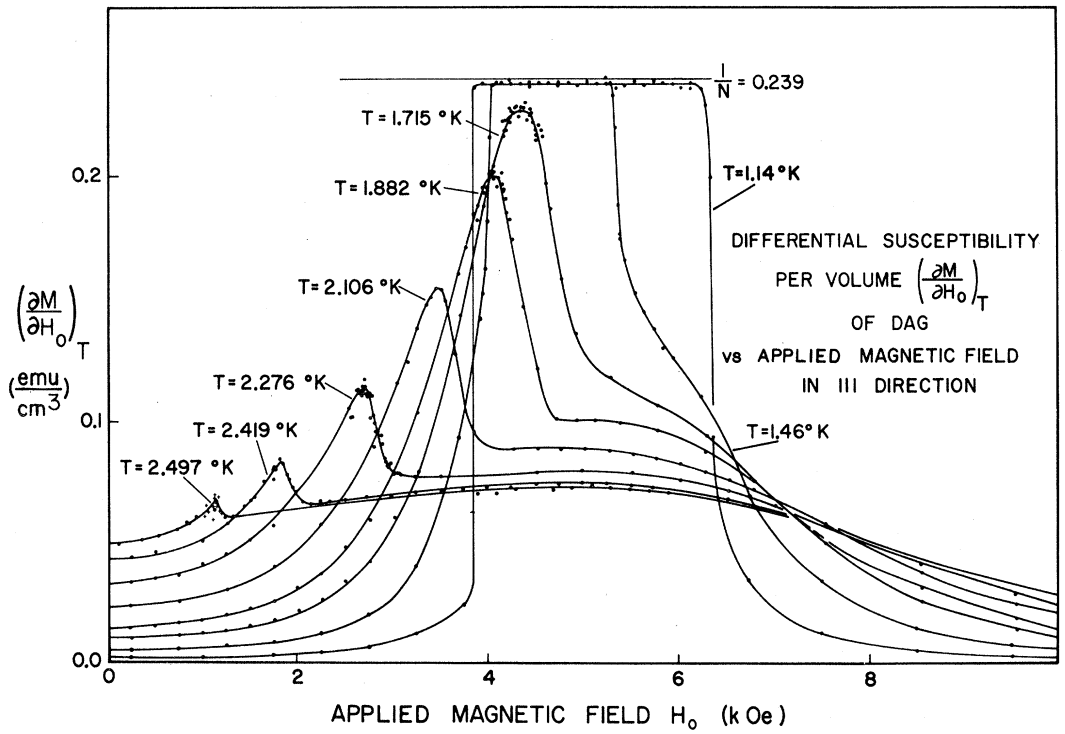

FIG. 4. Differential susceptibility $(\partial M/\partial H_0)_T$ of a DAG sphere as a function of applied field H_0 along [111] for $T < 2.50$ °K. For temperatures above $T_t = 1.66$ °K well-defined rounded maxima corresponding to a "higher-order" phase transition can be seen, but for $T < 1.66$ °K the curves show a field- and temperature-independent region close to the theoretical value $1/N = 0.239$ corresponding to a first-order phase transition.

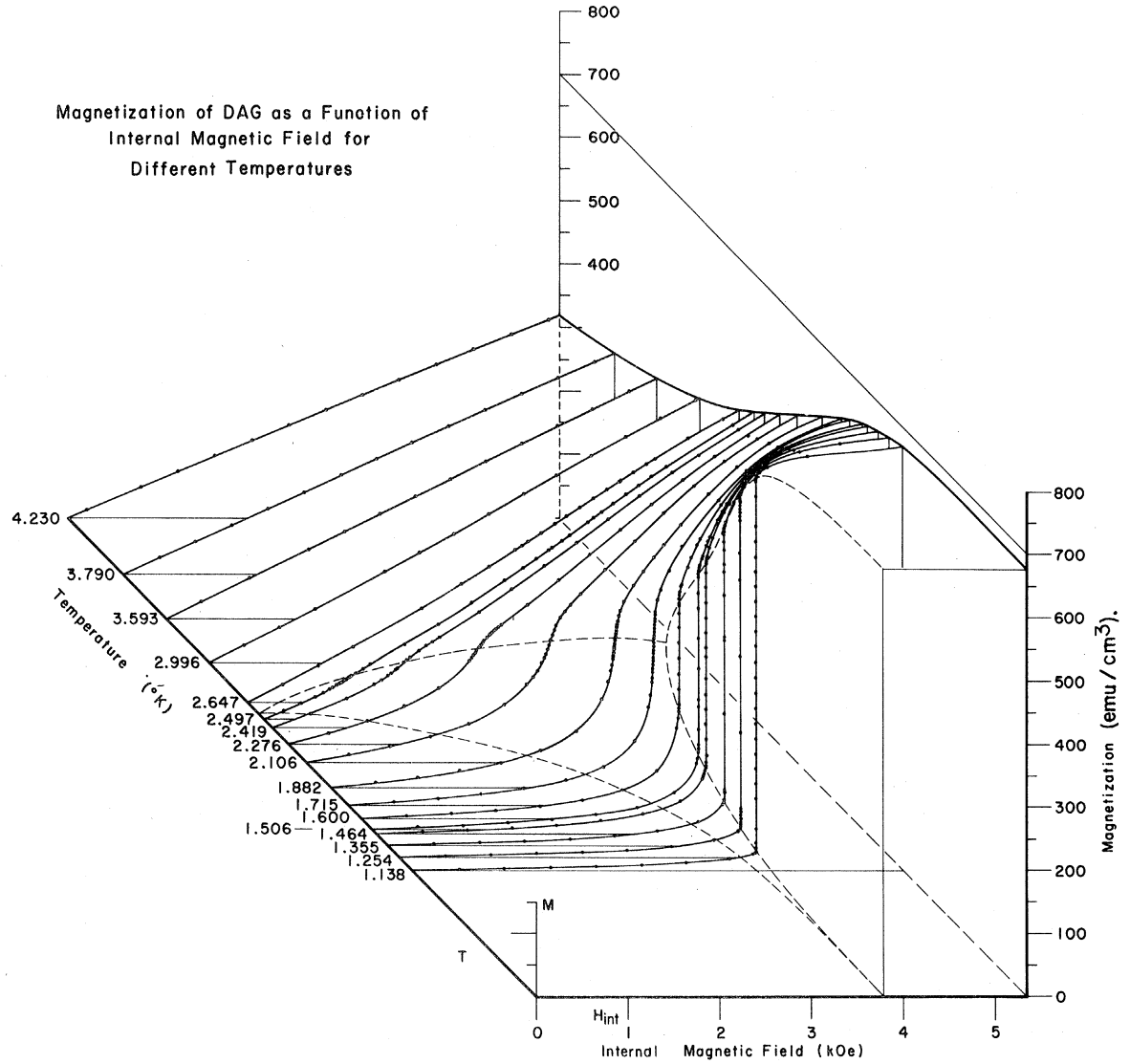

FIG. 5. Isothermal magnetization of DAG as a function of *internal* magnetic field H_i along [111] and temperature.

ials this effect might well be more important.

We can conclude that the observed transition in DAG below 1.66 °K is rather accurately described as a simple first-order phase change if the correction for demagnetizing effects is made macroscopically, treating the system as effectively homogeneous.

At very low fields the magnetization tends to zero with H_0, and by plotting M/H_0 as a function of H_0^2 we can extract values for the zero-field susceptibility χ_0. These may be compared with the *ac* susceptibility measurements reported previously,[1] and as we might expect, the two methods give the same result within experimental error. This shows that the effective relaxation time in the antiferromagnetic state is less than about 10^{-3} sec, which is not surprising since in zero field only spin-spin relaxation is important.[62]

2. $1.66 < T < 2.53$ °K

In this range the magnetization isotherms show no sharp singularities, but on each curve there is a marked inflection which corresponds to a well defined but smooth peak in $(\partial M/\partial H_0)_T$ (Fig. 4). The positions and heights of these peaks vary with temperature. As T tends towards 2.53 °K, which is the zero-field Néel point (see Sec. IV), the peaks get smaller and move towards zero field. As T decreases, the peaks grow until they reach their limiting height of $1/N$ at 1.66 °K. Expressed in terms of H_i the peaks are sharper (Fig. 7) but the general behavior is similar.

At this time there is no theoretical model which predicts properties of this kind. We shall defer the

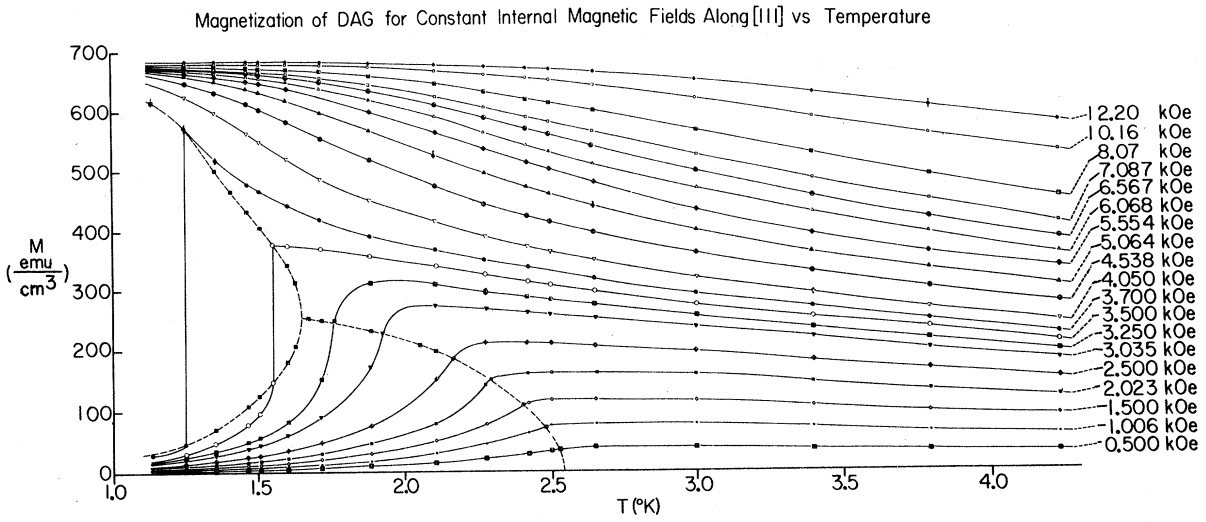

FIG. 6. Magnetization of DAG as a function of temperature for constant *internal* fields H_i along [111]. The broken line indicates the antiferromagnetic-paramagnetic phase boundaries which are shown in more detail in Fig. 12.

discussion of the available models until a later time, but for the present we must note that there is no rigorous way of identifying the precise location of any phase transition from the observed curves. It seems intuitively clear that the peaks are related to the antiferromagnetic-paramagnetic phase transition already identified below 1.66 °K but the nature of the phase transition is unusual. Since both M and

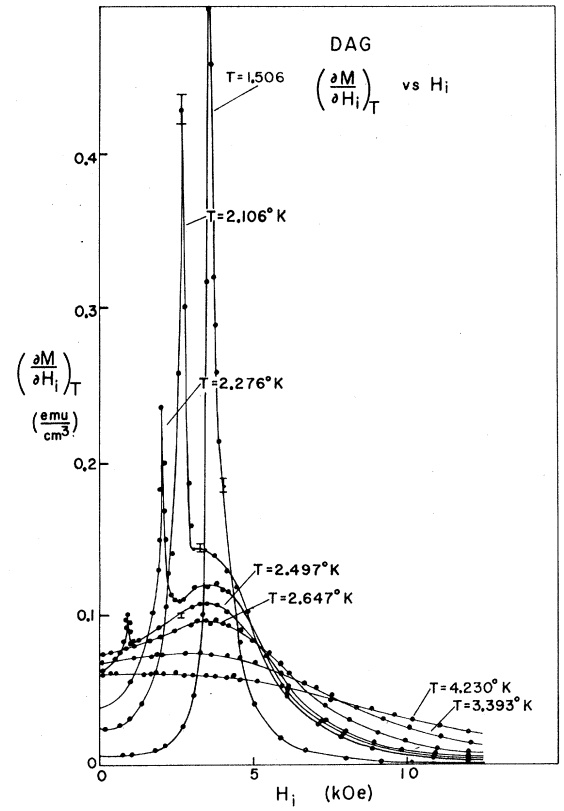

FIG. 7. Differential isothermal susceptibility $(\partial M/\partial H_i)_T$ of DAG, corrected to a sample shape corresponding to $N=0$, as a function of H_i along [111].

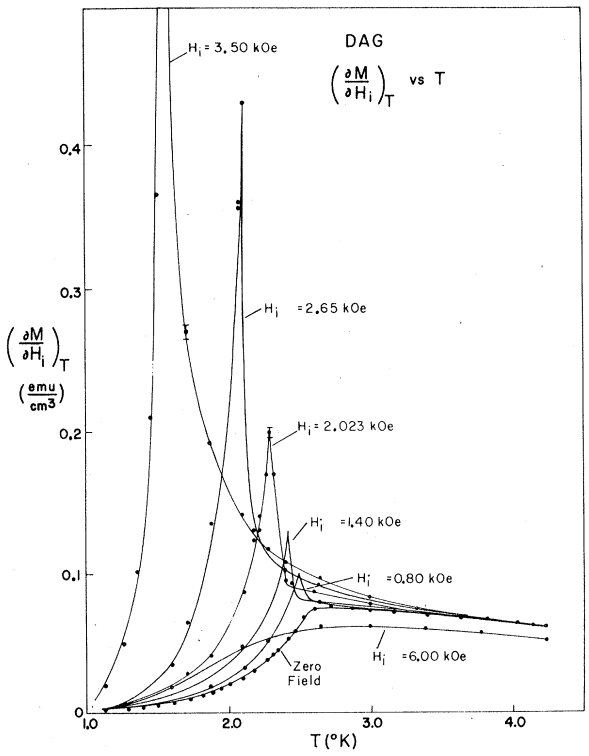

FIG. 8. Differential isothermal susceptibility $(\partial M/\partial H_i)_T$ of DAG as a function of temperature for fixed internal fields H_i along [111], corrected to $N=0$.

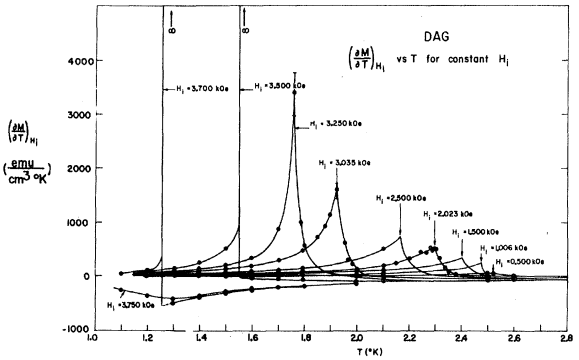

FIG. 9. Variation of $(\partial M/\partial T)_{H_i}$ for DAG as a function of temperature for fixed H_i along [111].

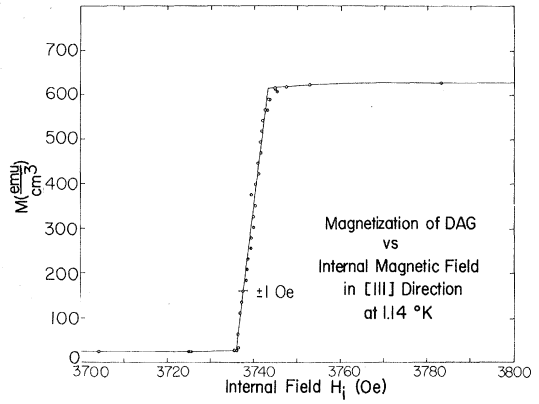

FIG. 11. Expanded plot of the magnetization isotherm at $T = 1.14$ °K showing the accurate linearity in the region of the first-order phase transition. The small deviation from the vertical is readily explained by a 0.3% error in the demagnetization correction.

$\partial M/\partial H$ are continuous in this range it is neither first *nor* second order and yet it grows gradually into a first-order transition at 1.66 °K. As a working approximation we shall tentatively identify the actual peak in $(\partial M/\partial H_0)_T$ as the point at which the symmetry changes from antiferromagnetic to paramagnetic[63] and refer to the phase change as simply of "higher order."[64,65] It is clear that further theoretical study of this type of situation is needed.

With this definition we can plot further sections of the phase boundaries on both the M-T and the H-T plots (Figs. 12 and 13). As we might anticipate, the curves join smoothly to the phase boundaries found below 1.66 °K. In particular the H_i^c-T curves join without any apparent discontinuity suggesting that the first-order transition is indeed a natural development of the higher-order phase change.

The junction of the three phase boundaries on the M-T plot at the tricritical point $(M_t,\ T_t)$ is also of interest and it is clearly reminiscent of a similar phase diagram for He^3-He^4 mixtures.[66] It is unfortunate that the phase boundaries in the present case are subject to difficulties of interpretation, experimental below $(M_t,\ T_t)$ and theoretical above,

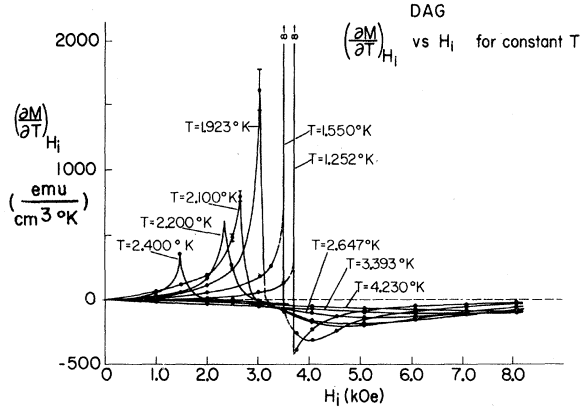

FIG. 10. Variation of $(\partial M/\partial T)_{H_i}$ for DAG as a function of internal field H_i along [111] for fixed temperatures.

and not too much emphasis should therefore be placed on the apparent differences in the way the curves join.

3. $T > 2.53$ °K

In this range DAG is paramagnetic for all magnetic fields and there are no further phase transitions. We may note, however, a broad peak in $(\partial M/\partial H_0)_T$ which gradually decreases in height and field as T increases until it disappears at about 3.8 °K. Closer inspection of the $(\partial M/\partial H_0)_T$ curves at lower temperatures reveals that this peak is not restricted to temperatures above 2.53 °K but is in fact present at all temperatures below 3.8 °K, though it ultimately becomes overshadowed by the much larger peak corresponding to the low-temperature phase transition. This is really not surprising since the broad peak is clearly a property of the paramagnetic phase and in the presence of a magnetic field this certainly persists below 2.53 °K.

To explain a peak in the paramagnetic phase we have to consider details of the spin-spin interactions and this is beyond our present scope. However, we can see qualitatively how such a peak can arise if we consider a situation in which there are relatively strong antiferromagnetic interactions which are such that they tend to cancel when the spins are aligned by a sufficiently strong magnetic field. In high fields the system then behaves like a simple paramagnet and $\partial M/\partial H_0$ decreases due to saturation. At lower fields the effect of the interactions becomes important and $\partial M/\partial H_0$ is again depressed, but now by the antiferromagnet short-range order. As the temperature increases the short-range order becomes weaker and the peak moves to lower fields until it ultimately disappears. The temperature at which this occurs corresponds to the "Boyle temperature" in the p-V diagram of

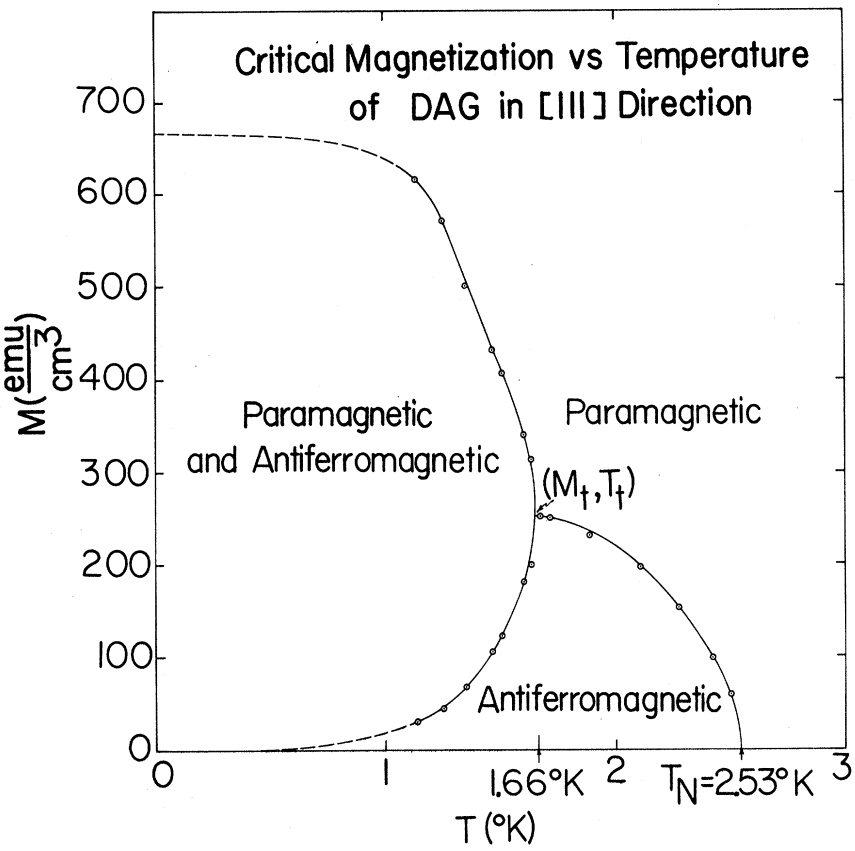

FIG. 12. Magnetic phase diagram of DAG in the M-T plane. For temperature between $T_N = 2.53$ °K and $T_t = 1.66$ °K, the phase boundary is tentatively identified by the maxima in $(\partial M/\partial H_0)_T$ and it appears to be of higher than second order. For temperature below $T_t = 1.66$ °K the phase boundaries are identified by the ends of the near vertical section on the M-H_i isotherms which indicate a first-order phase transition. Between the upper (M^+) and lower (M^-) branches the antiferromagnetic and paramagnetic phase are in coexistence.

a nonideal gas.[67] The peculiar features of interactions which cancel when the spins are aligned are here a result of the unusual structure of DAG and this will become apparent in II.

IV. THERMAL MEASUREMENTS: RESULTS AND DISCUSSIONS

A. Specific-Heat Measurements

One of the main problems in the interpretation of measurements on magnetic systems is the difficulty of separating magnetic and nonmagnetic contributions. In the present case this turns out to be unusually easy since the magnetic specific heats are generally large[68] (0.1 to $5R$) while the nonmagnetic lattice specific heat C_L is very small. In order to estimate C_L, specific-heat measurements were made on samples of $Y_3Al_5O_{12}$ (YAG) and $Lu_3Al_5O_{12}$ (LAG), and these are reported briefly in the Appendix. The results showed that $C_L \sim (10^{-5}T^3)R$, (T in °K), so that the lattice contribution was generally less than 1% of the total specific heat and often quite negligible. Where significant, a correction was applied and all the thermal data discussed in this section may be taken as purely magnetic properties.

In addition to simplifying the analysis of the experimental data, the small lattice specific heat reduces the possibility of complications arising from magnetoelastic effects. These can become important if magnetic and lattice energies are comparable, and prevent any meaningful separation of the purely magnetic properties. This complication is of particular interest in connection with high-resolution measurements in the immediate vicinity of critical points which can be modified profoundly by such effects.[69–71] For DAG we would expect these to be very small, and we might hope to find an unusually sharp λ anomaly, characteristic of a simple magnetic transition.

1. *High-Resolution Measurements in Zero Field*

High-resolution specific-heat measurements were made on all four large single crystals, as described in Sec. IIC. The results of a typical run for sample 1 (the shaped ellipsoid) covering four decades of temperature resolution are shown in Fig. 14. To avoid any prejudice in interpretation the results have been plotted on a linear scale with temperatures expressed in terms of an arbitrarily chosen T_{max}. Since temperature differences can be measured much more accurately than absolute temperatures this also avoids major calibration difficulties. Smoothed values C/R versus T-T_{max} for sample 1 are given in Table I. The results for other samples were very similar, and a comparison showing the results for three of these samples has been given in one of our earlier reports.[10,72]

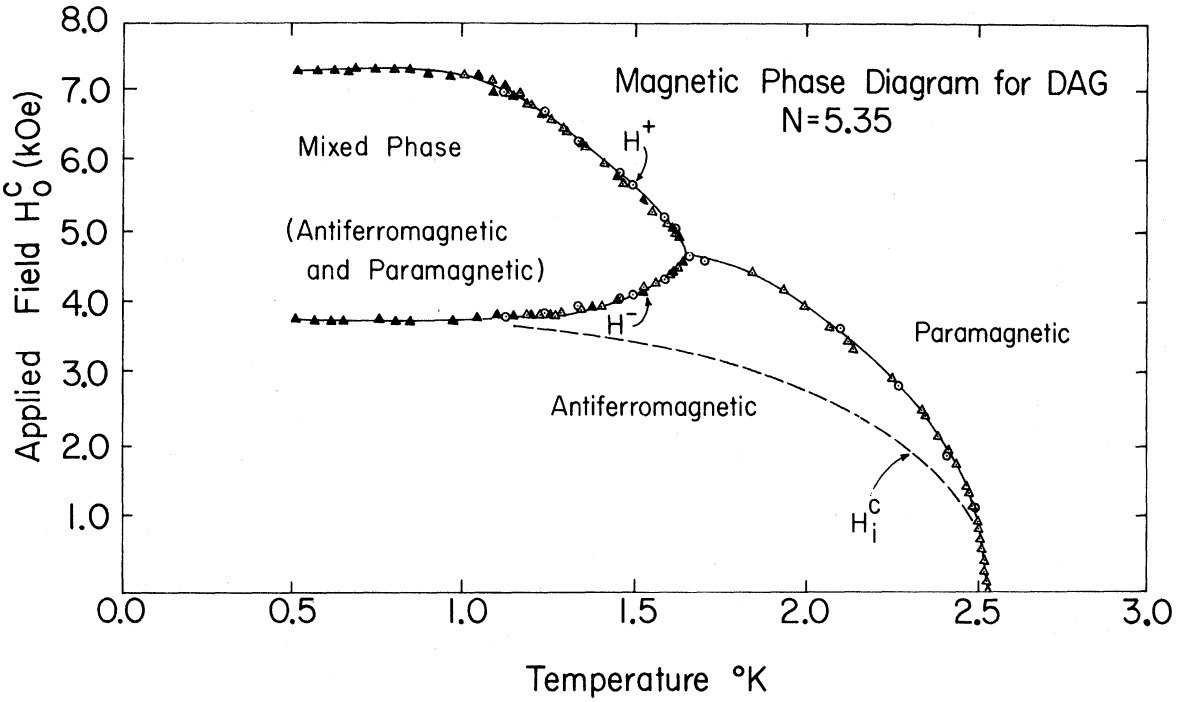

FIG. 13. Magnetic phase diagram for DAG in the H_0-T plane for a sample corresponding to $N-5.35$: circles are the magnetic measurements corresponding to the data shown in Fig. 12; open triangles are the maxima of C_H-T curves shown in Figs. 15–17; closed triangles are the end points of first-order transition determined from isothermal field sweeps (see Fig. 19). The broken line is the phase boundary calculated from the experimental data for the case of $N=0$. Within the limits of experimental accuracy (±10 Oe) this curve shows no kink at the tricritical temperature T_t = 1.66 °K.

The peaks in all cases were rounded over about 2 m °K and showed no obvious features which indicate the ordering temperature. The rounding corresponds to $\epsilon=(T-T_N)/T_N\sim 4\times10^{-4}$ which is comparable to the sharpest λ anomalies which have been reported[73–75] for magnetic materials, and the peak heights (4.2 to 5.1R) were also among the largest which have been found. It thus appears that DAG is as good as, but no better than, other materials for studying critical phenomena. On the other hand, it is interesting that four completely different samples showed almost identical rounding in the region of T_N, suggesting that the broadening of the λ peak may perhaps be an intrinsic property in the case of DAG, and not the result of impurities or defects which would surely be somewhat different for crystals grown at widely spaced times, albeit by the same method.

An indication that the four crystals were not in fact quite identical was found in the fact that the temperatures at which the peaks occurred were not exactly the same. To check that this was not an experimental artifact resulting from incorrect temperature calibrations we made a composite sample

TABLE I. Smoothed specific heat of DAG sample 1 in the region of T_N. Temperatures are measured relative to an arbitrarily chosen T_{max}=2.544 °K, close to the temperature of the observed maximum. T_N may be about 1 m °K above T_{max}.

$T-T_{max}$ (m °K)	C/R	$T-T_{max}$ (m °K)	C/R	$T-T_{max}$ (m °K)	C/R
−200.0	1.54	−1.0	4.30	2.0	1.60
−150.0	1.78	−0.5	4.53	5.0	1.29
−100.0	2.04	−0.2	4.81	10.0	1.08
− 50.0	2.41	−0.1	4.95	15.0	0.96
− 20.0	2.92	0	5.08	20.0	0.89
− 15.0	3.08	0.1	4.80	50.0	0.66
− 10.0	3.14	0.2	4.51	100.0	0.50
− 5.0	3.61	0.5	3.50	150.0	0.42
− 2.0	4.14	1.0	2.50	200.0	0.39
− 1.5	4.20	1.5	1.75		

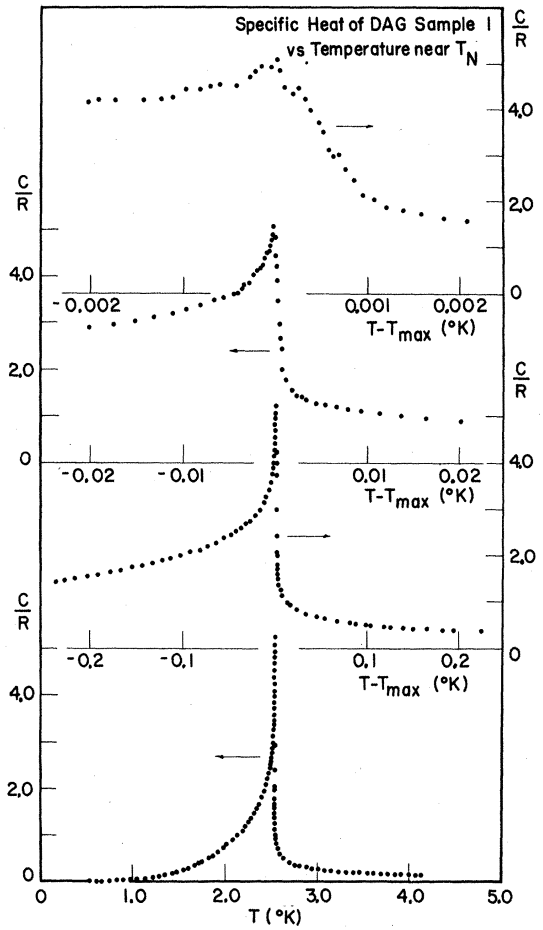

FIG. 14. Specific heat of DAG sample 1 as a function of temperature near T_N, under four decades of temperature resolution. Temperatures are measured relative to an arbitrarily chosen $T_{max}=2.544$ °K. Smoothed values corresponding to these curves are given in Table I.

consisting of three of the single crystals in thermal contact and measured the total heat capacity. The results[8] were as expected from the separate measurements, the total heat capacity showing three peaks at temperatures spread over a range of 23 m °K, a difference ten times larger than the widths of the individual peaks.

We have not been able to find any significant differences in any other properties which might explain this spread of ordering temperatures (see Sec. II A) but it seems most likely that small variations in the stoichiometry are in fact responsible. It is not clear whether these could also account for the peak widths, but this seems less likely since the widths are about the same in all the samples.

In view of these difficulties it is important to ensure that magnetic and thermal data which are to be compared or combined are either made on the same sample, or, where this is not convenient, on two samples with similar T_N's. We were thus fortunate to find that our spherical magnetometer sample had a T_N of 2.540 °K, as indicated by the zero of H-T phase boundary, while the large ellipsoid for the thermal measurements has its specific-heat peak at $T_{max}=2.544$ °K. Gaunt and Domb[76] have argued that the actual T_N is in fact slightly above T_{max} (~0.001 °K), but in any case the agreement is quite close.

2. *Specific-Heat Measurements in Constant Applied Fields*

Measurements were made in fields ranging from 1 to 14 kOe at temperatures between 1.2 and 4.2 °K. A striking variety of results was found, as shown in Figs. 15–18.

For low fields, sharp λ-like peaks were observed whose height decreased as their width increased with H. If we take the peaks as indicating the antiferromagnetic-paramagnetic transition we can plot a series of points on the H_0-T phase diagram and these are shown in Fig. 13. Once the phase boundary was established approximately, it was easy to make a large number of additional specific-heat measurements over short temperature ranges to locate the phase boundary precisely and these points are also shown in Fig. 13. It can be seen that the agreement with the point determined from the peaks in $(\partial M/\partial H_0)_T$ is very good. The shape of the phase

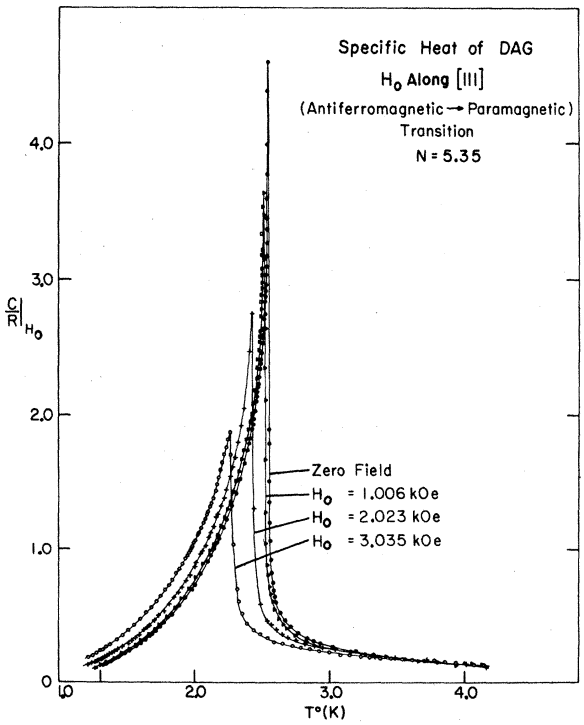

FIG. 15. Specific heat of the DAG ellipsoid ($N=5.35$) as a function of temperature in constant applied fields H_0 along [111] showing the shift of the paramagnetic-antiferromagnetic phase transition for fields up to 3 kOe.

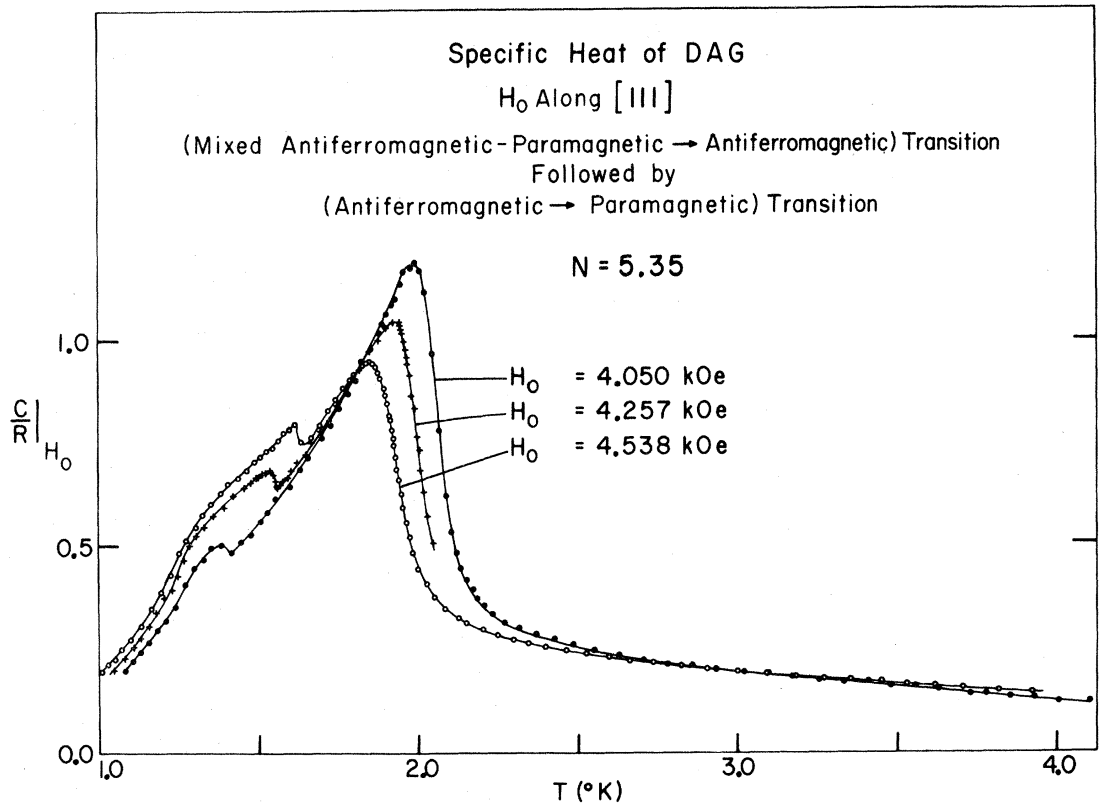

FIG. 16. Specific heat of the DAG ellipsoid ($N=5.35$) as a function of temperature in constant applied fields H_0 along [111] showing the transition from the mixed antiferromagnetic-paramagnetic state of the simple antiferromagnetic state (lower-temperature peaks), followed by the antiferromagnetic-paramagnetic transition (higher-temperature peaks).

boundary as $T \to T_N$ will be discussed in II.

For fields in the range 3.8–4.7 kOe quite unusual double-peaked specific-heat curves were found, as shown in Fig. 16. The origin of these is readily understood if the peak positions are plotted on the phase diagram already established from the magnetic measurements. It can then be seen that lower peaks correspond to crossing the lower branch of the first-order coexistence boundary, H_0^-, while the upper peaks correspond to the "higher-order" antiferromagnetic-paramagnetic phase change. The broad and asymmetrical shape of these peaks results from the fact that the measurements are made at constant *external* fields, and we shall show in Sec. VI that these effects disappear if the results are expressed in terms of the internal field H_i.

For fields between 4.7 and 7.1 kOe the curves were again different in character (Fig. 17) but this behavior can also be understood in terms of the H_0-T phase diagram. The peaks now correspond to a crossing of the upper branch, H_0^+-T, from the mixed antiferromagnetic-paramagnetic state to the simple paramagnetic phase. For points corresponding to the mixed state, the specific heat at constant external field has very little direct meaning, since a temperature change at constant H_0 implies a change in the relative concentration of the two phases, so that the measured heat capacity is really a combination of latent heat and specific heat. An analysis along these lines will be discussed in Sec. VI.

For a sample with $N=5.35$ there is no phase transition in fields above about 7.2 kOe, and the specific-heat curves for higher fields would be expected to show purely paramagnetic behavior, corresponding to a simple splitting of the ground state in the field only slightly modified by the interactions. The results in Fig. 18 show that this is indeed found. The curves are all smooth, with peak values almost independent of H and equal to about $0.44R$, as for a simple Schottky anomaly. A detailed analysis given in II shows that the fit to the Schottky form is quite good especially at the lowest temperatures and highest fields, as one might expect.

B. Magnetocaloric Measurements

Associated with the first-order magnetic phase transition below 1.66 °K, there is a latent heat $L(T)$ which can be measured by means of isothermal field sweeps as described in Sec. IID. It turns out that the magnetocaloric effect also provides an ex-

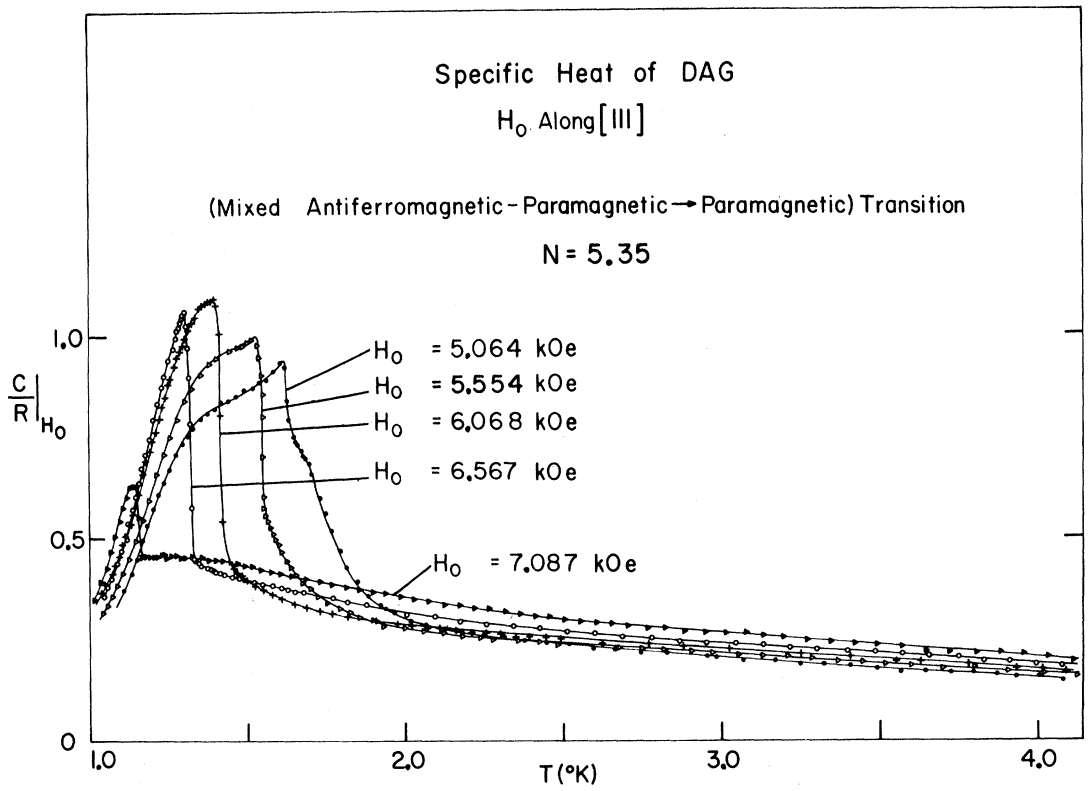

FIG. 17. Specific heat of the DAG ellipsoid ($N=5.35$) as a function of temperature in constant applied fields H_0 along [111] between 5.0 and 7.1 kOe. In this region the phase boundary is crossed only once, corresponding to a transition from the mixed antiferromagnetic-paramagnetic state to the paramagnetic state.

cellent way of locating the phase boundaries of the mixed state, especially at the lowest temperatures where other methods become difficult.

In the paramagnetic region $(\partial T/\partial H)_S$ is generally positive and decreasing the magnetic field tends to cool the sample. A positive supply of electrical heat $\dot{Q}$ is therefore required to maintain a constant temperature as the field is reduced [see Fig. 19(a)]. This may be contrasted to the behavior in the antiferromagnetic state where the heat is required as the field is *increased* [see Fig. 19(b)–19(d)]. When the system enters into the mixed antiferromagnetic-paramagnetic state, corresponding to the first-order transition in a finite sample, neither of these two effects is important, since the internal field remains *constant* in this region, and as the external field is increased there is simply a gradual transformation of the antiferromagnetic phase into the paramagnetic phase. In order to maintain a constant temperature, a supply of electrical heat proportional to the latent heat of transformation is then required. If the end points of the transformation can be identified, $L(T)$ is readily found by integrating

$$\int_{H_0^-}^{H_0^+}\left[\dot{Q}\Big/\left(\frac{dH_0}{dt}\right)\right]dH_0 = L(T)\ . \tag{6}$$

To a good first approximation this turns out to be rather easy. The sweep rate dH/dt can be held at an essentially constant value and since the amount of paramagnetic phase in the mixed state is directly proportional to H_0-H_0^-, (as evidenced by the linear M-H_0 curves), $\dot{Q}$ should be quite constant between H_0^+ and H_0^-. Outside this region the usual magnetocaloric effects take over and $\dot{Q}$ should again vary with H_0. Figures 19(c) and 19(d) show that this is essentially what is found. $\dot{Q}$ is indeed constant over a broad region coinciding with the mixed state, but not too surprisingly there are small deviations at both ends. These can be understood readily in terms of two simple effects.

Firstly, the mean internal field could easily deviate from its constant value when one of the two phases occupies only a very small fraction of the sample volume. Under this condition the assumption of homogeneity will not be such a good approximation and different regions of the sample may experience somewhat different fields. The second effect, which appears to be important only as the system enters into the mixed phase region, is a small lag in the response, corresponding to supercooling. Both these effects are quite small, extending over only 30 Oe or so, and it should be fairly accurate to estimate ideal behavior by visual

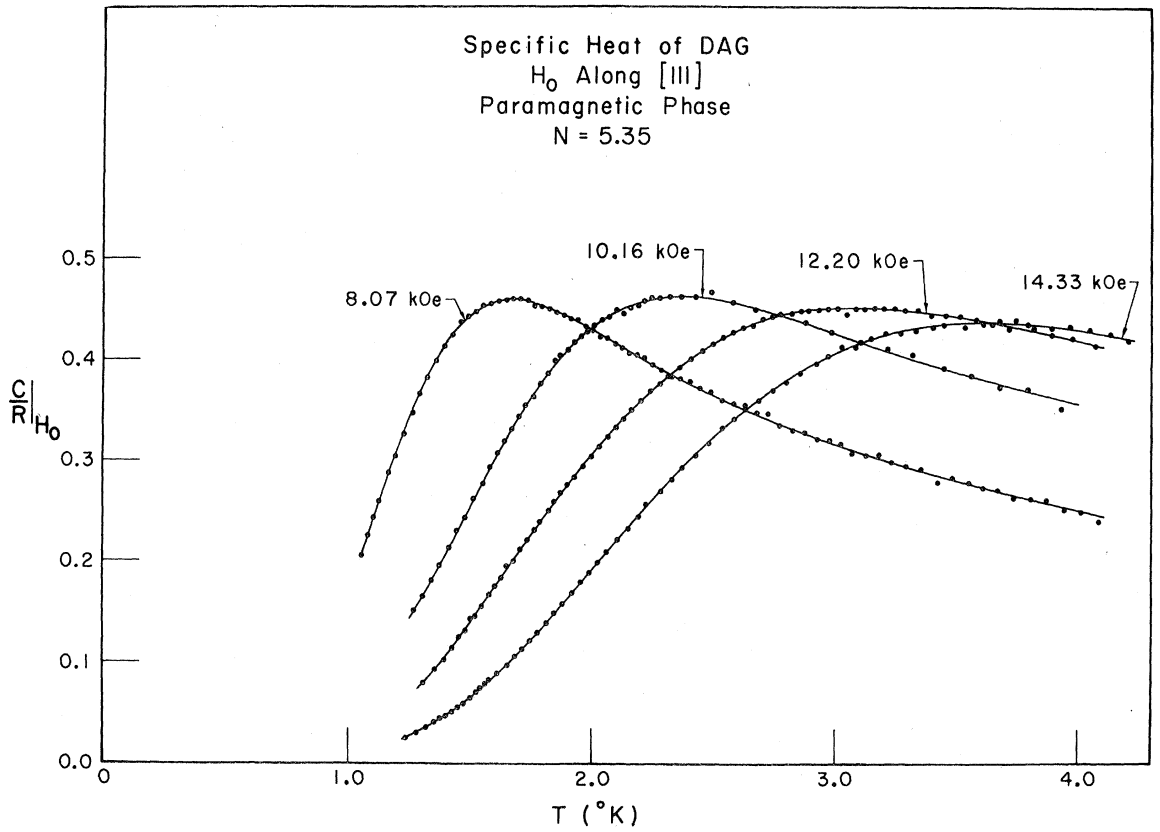

FIG. 18. Specific heat of the DAG ellipsoid ($N=5.35$) as a function of temperature in constant applied fields H_0 along [111]: $H_0=8.07$, 10.16, 12.20, and 14.33 kOe. For these fields the sample remains in the paramagnetic phase at all temperatures.

extrapolation, as indicated in Fig. 19. This could be checked by comparing the estimated end points against the phase diagram already established by the two other methods, where these overlap with the magnetocaloric data (see Fig. 13). The agreement is seen to be excellent, and it gives support to the points below 1.1 °K where no data are available from the other methods.

Using the same extrapolation to remove the end effects we can now estimate $L(T)$ from Eq. (6). The results are shown in Fig. 20. It can be seen that $L(T)$ goes to zero at 1.66 °K, as it should, and it also becomes small at low temperatures as one might expect. Figure 20 also includes a plot of $-T(M^+-M^-)\partial H_i^c/\partial T$ estimated from the magnetization data, which is the Clausius-Clapeyron expression for the latent heat. The agreement over the entire range is quite good.

The agreement between the thermal and magnetic determinations of $L(T)$ gives support to an implicit assumption which requires some justification. We have assumed that $\dot{Q}$ in Eq. (6) is measured entirely by the electrical heat supplied to the sample and that heating due to both elastic changes and irreversible processes are negligible. Magnetoelastic changes might indeed be thought to be small since the magnetic interactions are rather weak and not too sensitive to volume.[77] Heating from irreversible processes, on the other hand, would not be at all unreasonable since the transformation proceeds by growth of domains and such changes are never really reversible. Evidence that irreversible heating does in fact occur was obtained from field sweeps at temperatures below 0.7 °K where $L(T)$ is very small. It was found that the sample temperature increased without electrical heating for both increasing and decreasing field sweeps. However, the effect was not very big and it would probably be even smaller at higher temperatures.

In order to ascertain in what regions irreversibilities might occur and obtain estimates of the corresponding heating, we have carried out a series of adiabatic magnetization-demagnetization cycles. In each cycle the initial and final fields were the same and the total amount of irreversible heating could be estimated from difference in initial and final temperatures and the measured specific heat C_{H_0}. The results are given in Table II. It can be seen that the change of entropy $\Delta S/R$ is generally fairly small, especially at the higher temperatures

and in cycles which do not involve the mixed state. At the lowest temperatures the irreversible heating becomes comparable to the measured latent heat and may introduce a significant error. Unfortunately, there is no way of correcting for this effect from the available data since adiabatic and isothermal field sweeps follow quite different paths, and it seems clear that a more detailed study of these effects is required.

For the present we can conclude that the latent heat associated with the first-order phase transition is probably given quite accurately (± 10%) by Fig. 20 down to about 1.1 °K, and it seems likely that it will tend to zero monotonically (i.e., without changing sign) as T goes to zero. Additional confirmation of the latent heat measurements will be obtained from the entropy determinations described in Sec. V.

V. DERIVED THERMODYNAMIC FUNCTIONS

Given the results of measurements of both M and C_{H_0} as a function of H_0 and T it is in principle possible to find all other thermodynamic functions. A small difficulty in practice is that measurements are possible over only a finite range of temperatures, and in order to put thermodynamic functions on an absolute basis, extrapolations to $T=0$ or ∞ are needed. In the present case these extrapolations turn out to be quite small and they can be made rather accurately since the forms of the high- and low-temperature behavior are known from the theoretical model for DAG (see Paper II). It is thus possible to obtain an unusually complete picture of the magnetothermodynamic behavior over the entire range of temperature and field, and to make the kind of thermodynamic study usually possible only for liquid-gas systems, with the additional advantage that the results can be related directly to an accurate microscopic model[78–85] (see Papers II and IV).

A. Entropy and Energy in Zero Field

With no applied field present the entropy S/R and the internal energy U/R could be determined direct-

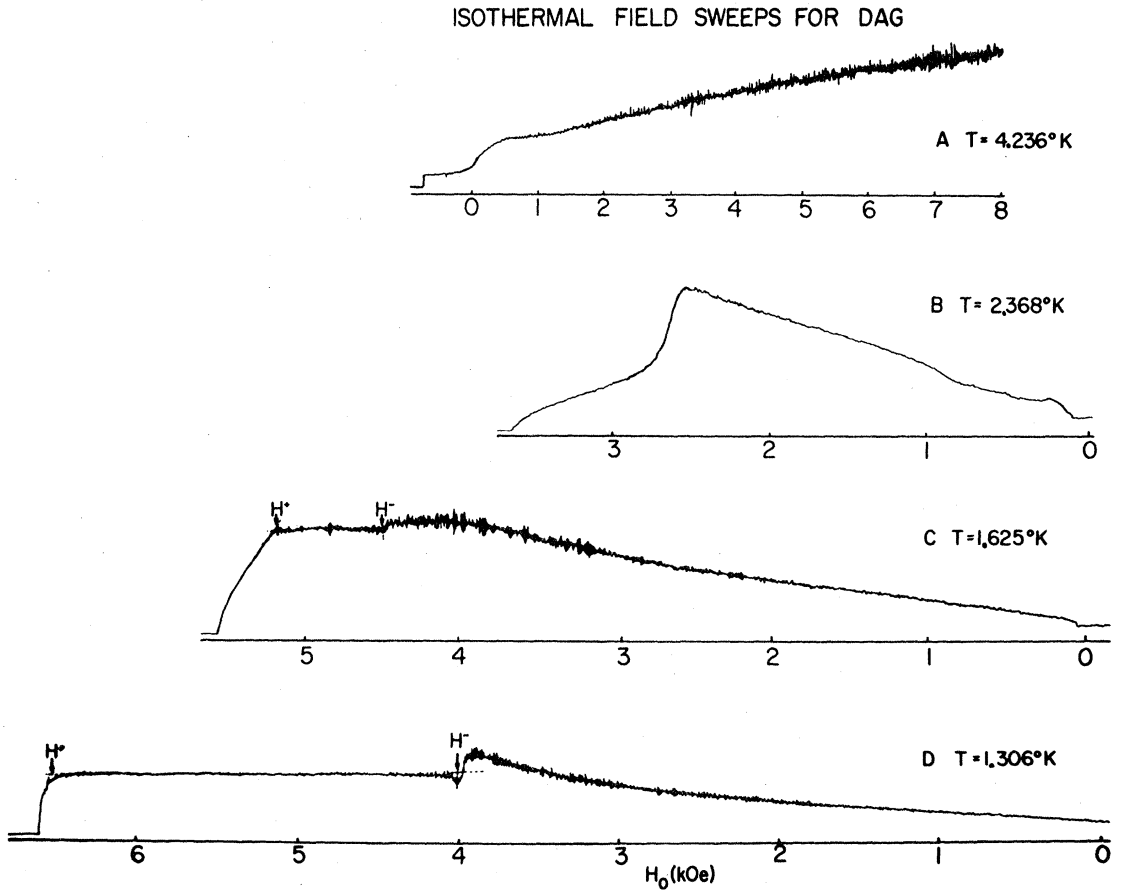

FIG. 19. Experimental results of a series of isothermal field sweeps for temperatures between 1.3 and 4.4 °K: (a) $T=4.336$ °K; (b) $T=2.368$ °K; (c) $T=1.625$ °K; (d) $T=1.306$ °K. For all the sweeps the time increases in going from right to left regardless of whether the field is increasing or decreasing. H^+ and H^- mark the upper and lower boundaries to the mixed phase region. The dashed lines correspond to the extrapolated heat input corrected for "end effects."

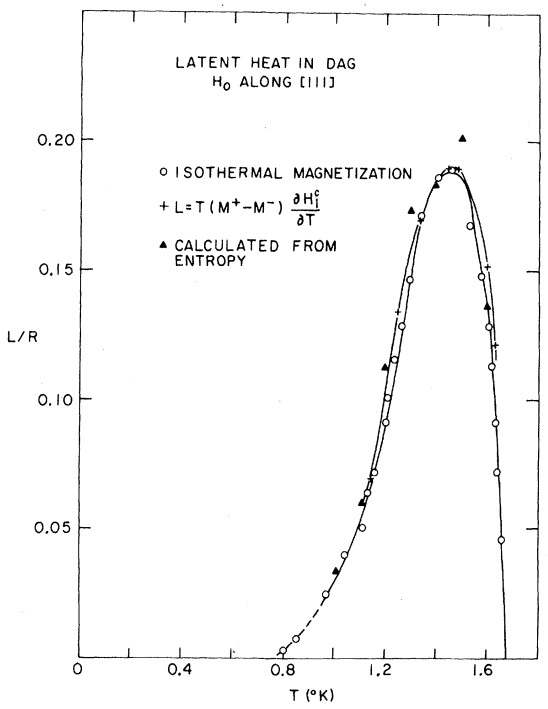

FIG. 20. Latent heat of DAG associated with first-order phase transition in fields along [111]. Open circles are the values determined by integration of heat input during isothermal magnetization; pluses are the values calculated from magnetic Clausius-Clapeyron equation $L=-T(M^+-M^-)\,\partial H_i^c/\partial T$; closed triangles are the values calculated from entropy curves using Eq. (9).

ly from the specific heat, using the relationships

$$\frac{S}{R}=\int_0^T \frac{C}{RT}\,dT\,, \tag{7a}$$

$$\frac{U}{R}=\int_\infty^T \frac{C}{R}\,dT\,, \tag{7b}$$

where the scales are chosen such that $S/R=0$, where $T=0$, while $U/R=0$ when $T=\infty$. The major contribution to both these integrals comes from the range $T=1.3$–$4.2\,^\circ$K for which the most detailed measurements have been made. The results obtained for this range are shown in Figs. 21 and 22. To facilitate the extrapolations to $T=0$ and $T=\infty$ some additional specific-heat measurements were made down to $0.55\,^\circ$K and up to $8\,^\circ$K. Between 0.55 and $1.3\,^\circ$K the specific heat could be fitted to a law of the form $C/R=b/T^2+(\Delta/T)^2e^{-\Delta/T}$, where the first term is primarily due to nuclear effects and the second represents the magnetic specific heat (see II).[86] Using the fitted value of Δ, the magnetic entropy change could be estimated as

$$(\Delta S/R)_{0\to 1.3\,^\circ\mathrm{K}}=0.024\pm 0.001\,,$$

while the internal energy contribution was

$$(\Delta U/R)_{0\to 1.3\,^\circ\mathrm{K}}=(0.021\pm 0.001)\,^\circ\mathrm{K}\,.$$

The high-temperature extrapolations are more difficult to estimate since the lattice contributions become important above $4.2\,^\circ$K while the magnetic specific heat does not approach a simple asymptotic

TABLE II. Results of adiabatic field sweeps with $\vec{H}_0\parallel[111]$ in DAG. T_i and T_f are initial and final temperatures, and $H_i=H_f$ are the initial and final fields. $T_{\min}$ is the minimum temperature achieved during an individual sweep and corresponds approximately to the point of entry into a new phase region. H_m is the value of H at which the direction of the sweep was reversed.

T_i (°K)	T_f (°K)	$H_i=H_f$ (kOe)	Nature of sweep[a]	$T_{\min}$	H_m (kOe)	$\Delta S/R$
3.185	3.185	0	$P\to P\to P$	b	6.20	0.000 ± 0.005
3.90	4.03	6.14	$P\to P\to P$	2.650	0	0.006 ± 0.005
3.236	3.285	6.18	$P\to A\to P$	2.228	0	0.003 ± 0.005
2.127	2.150	6.11	$P\to A\to P$	1.874	0.40	0.004 ± 0.005
2.525	2.552	6.08	$P\to A\to P$	1.295	2.15	0.003 ± 0.005
1.531	1.534	6.12	$P\to A\to P$	1.205	0	0.007 ± 0.005
1.368	1.418	6.10	$P\to A\to P$	1.120	0	0.013 ± 0.005
1.540	1.630	0	$A\to P\to P$	1.048	5.90	0.018 ± 0.005
1.500	1.685	0	$A\to P\to A$	1.056	5.98	0.033 ± 0.010
1.638	1.760	0	$A\to P\to A$	1.047	6.00	0.026 ± 0.005
1.178	1.249	6.02	$P\to A\to P$	1.018	0	0.020 ± 0.005
1.210	1.281	6.10	$P\to A\to P$	1.023	0	0.020 ± 0.005
1.160	1.230	6.10	$P\to A\to P$	1.010	0	0.020 ± 0.005
1.158	1.231	6.11	$P\to A\to P$	1.010	0	0.021 ± 0.005
1.210	1.362	6.10	$P\to A\to P$	0.962	0	0.041 ± 0.010
1.170	1.563	0.37	$P\to A\to P$	0.929	6.02	0.045 ± 0.010
1.102	1.491	0	$A\to P\to A$	0.841	6.30	0.038 ± 0.010

[a] P indicates paramagnetic and A indicates antiferromagnetic phase.

[b] During this sweep the system remained paramagnetic with $(\partial T/\partial H_0)_S>0$; therefore, the sample immediately warmed as the field was increased and returned to its initial temperature only when the field was reduced to zero.

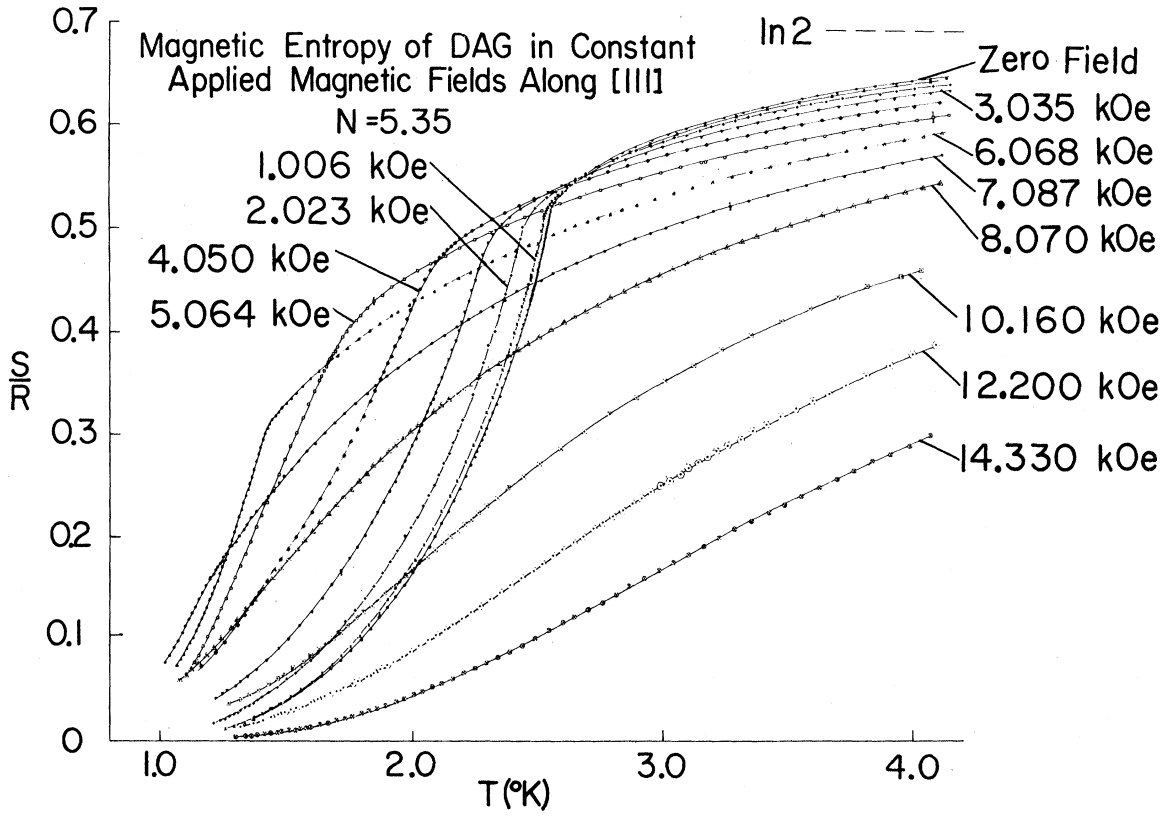

FIG. 21. Magnetic entropy of DAG as a function of temperature for constant applied fields H_0 along [111] in a sample with $N=5.35$.

form until about 6 °K. Estimating the lattice contributions as discussed in the Appendix, one can fit the magnetic specific heat between 6 and 8 °K to a high-temperature law of the form $C_2/T^2+C_3/T^3$ and hence estimate the entropy and energy contributions from the temperature range above 8 °K;

$$(\Delta S/R)_{8^\circ K\to\infty}=0.016\pm0.002\,,$$

$$(\Delta U/R)_{8^\circ K\to\infty}=0.23\pm0.03\,.$$

Between 8 and 4.2 °K the contributions can be found by direct numerical integration of the data corrected for the lattice specific heat.

Combining these extrapolations with the main parts given in Figs. 21 and 22 one can relate each curve to its appropriate zero, and one can estimate the total entropy change between zero and infinity. For the entropy one finds

$$(\Delta S/R)_{0\to\infty}=0.702\pm0.010\,,$$

in excellent agreement with the value $\ln 2=0.693$ expected for system with an effective spin $S'=\frac{1}{2}$.

For the total energy change one finds

$$(\Delta U/R)_{0\to\infty}=(1.92\pm0.05)^\circ K\,,$$

which may be compared with the value 1.89 ± 0.02 found from various estimates of the low-temperature excitation spectrum (see II).

Our estimates for both $(\Delta S/R)_{0\to\infty}$ and $(\Delta U/R)_{0\to\infty}$ are also in good agreement with earlier values[6] for which the error limits were rather larger.

B. Entropy in Applied Fields

In the presence of a field, entropy *changes* can be measured just as for zero field, but the determination of the appropriate absolute values is more difficult. Due to the transitions which take place at low temperatures, it is not possible to give a simple form for the variation of C_{H_0} as T tends to 0 °K while the high-temperature extrapolation is complicated by magnetoresistance effects in the thermometer which make calibration above 4.2 °K difficult.

To relate the different entropy curves to a common zero, we have therefore used an additional experiment, measuring the isothermal heat of magnetization at a temperature in the paramagnetic region. The arrangement was identical to that used to measure the latent heat, and the results expressed in terms of $(\partial S/\partial H_0)_{T=4.013}$ are shown in Fig. 23. Integrating, one can then find

$$S(H_0,T')=S(0,T')+\int_0^{H_0}\left(\frac{\partial S}{\partial H_0}\right)_{T'}dH_0\,, \qquad (8)$$

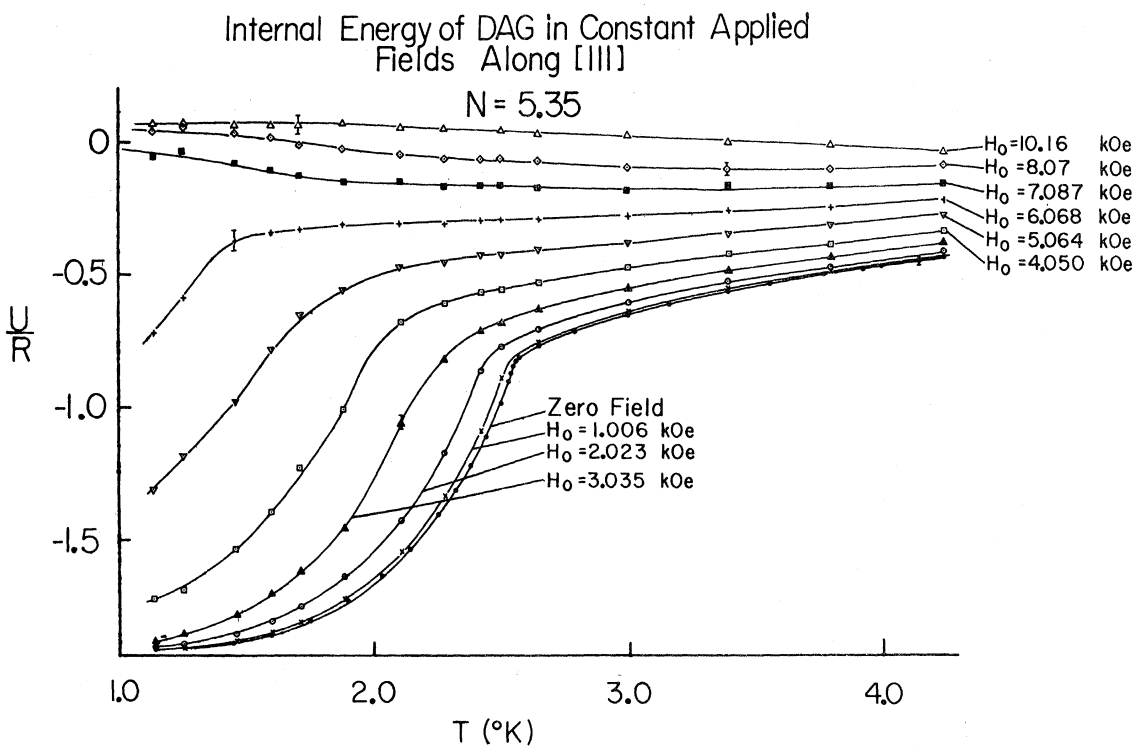

FIG. 22. Internal energy U/R of DAG as function of temperature for constant applied H_0 along [111], in a sample with $N=5.35$. The zero has been chosen so that $U/R \to 0$ as $T \to \infty$ for all H_0.

where $S(0, T')$ can be read off the previously determined zero-field curve (Fig. 21).

To check the accuracy of this procedure we attempted to compare $(\partial M/\partial T)_{H_0}$ estimated from our magnetic data with $(\partial S/\partial H_0)_T$. The results are shown in Fig. 23. It can be seen that the agreement at low fields is quite good, but at higher fields there appears to be a small systematic difference. The reason for this is not clear, but it is most probably due to errors in estimating small changes in M and applying the appropriate shape corrections. It may also be due to systematic errors in the en-

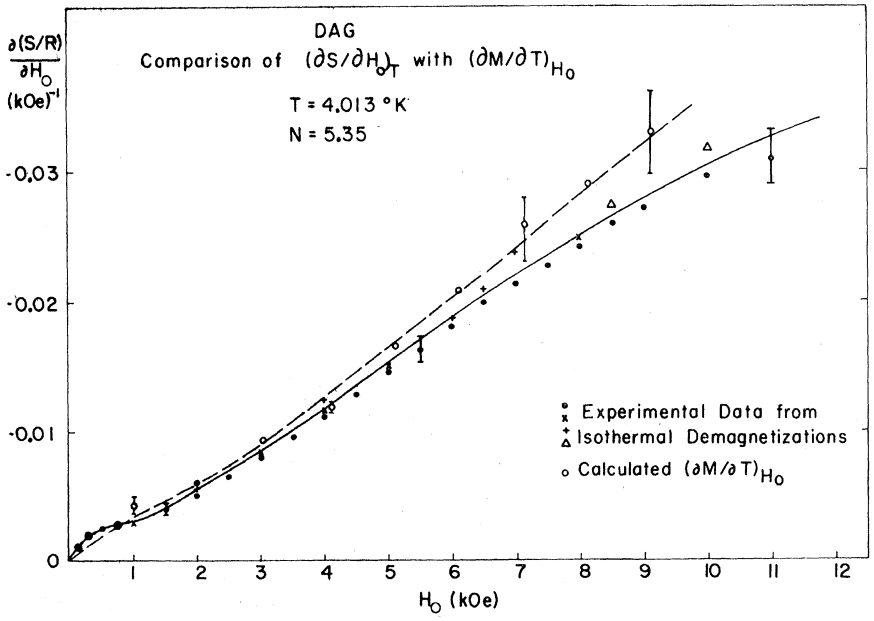

FIG. 23. Change of entropy with field, $(\partial S/\partial H_0)_T$ as a function of applied magnetic field H_0 along [111] at $T=4.013$ °K for a sample with $N=5.35$. Experimental data taken from different isothermal demagnetizations are shown as closed circles, crosses, pluses, and open triangles. The points shown as open circles are values of $(\partial M/\partial T)_{H_0}$ calculated from the magnetic data corrected to the same N.

tropy measurement arising from such effects as magnetoresistance in the thermometer or heater. In any case the discrepancy is really not very serious, since even up to 8 kOe, the total change in S is only $0.11R$, so that an uncertainty of 10% corresponds to an uncertainty in S of $0.01R$, or less than 2%.

For higher fields the error would be more important, but we can fortunately use another method for fields above about 8 kOe. In this range the specific heat approximates quite closely to a modified Schottky from (see Sec. IV A 2) and one can extrapolate to $T = 0\,^{\circ}\mathrm{K}$ as in zero field.

The results for all the entropy determinations are shown in Fig. 21. It can be seen that the behavior at high fields and high temperatures is generally very simple and consistent with our magnetocaloric experiments, but interesting complications can occur when the interactions become important. Thus a complex region is observed near $2.65\,^{\circ}\mathrm{K}$ where a number of curves cross, and we see, for example, that $(\partial T/\partial H_0)_S$ does not necessarily have to be positive throughout the paramagnetic phase, as it is away from the phase boundary. The change of sign of $(\partial T/\partial H_0)_S$ is thus not a good indication of a phase transition, as has sometimes been assumed.[79,84,87] Likewise $(\partial S/\partial H_0)_T$ is generally negative at high temperatures and positive in the antiferromagnetic state, but in a region such as that near $2.65\,^{\circ}\mathrm{K}$ almost anything can happen. Indeed an isothermal field sweep showed that $(\partial S/\partial H_0)_T$ changes sign *twice* near $2.65\,^{\circ}\mathrm{K}$ starting negative and ending negative, as the field increases. Such behavior is clearly the result of a competition between the field and interaction energies and it lends support for the anomalous looking bump at low fields shown in Fig. 23. To obtain further insight into these effects, additional experiments would certainly be required as the entropy differences are very small ($\sim 0.005R$) and comparable with the absolute accuracy of the present S-T curves ($\sim 0.007R$).

The entropy temperature curves can also be used to check the measured values of the latent heat $L(T)$. If we choose two points at the same temperature and at fields H_1 and H_2 which are both within the mixed phase region, we can calculate the latent heat from

$$L = T[S(H_2) - S(H_1)]\,(H^+ - H^-)/(H_2 - H_1)\,, \tag{9}$$

where we assume as before that the fraction of antiferromagnetic phase which would be transformed into paramagnetic in going isothermally from H_1 to H_2 is given by $(H_2 - H_1)/(H^+ - H^-)$. The results of this calculation at a number of temperatures are shown in Fig. 20, and it can be seen that the agreement is generally good. This lends further support to the assumption that irreversible effects do not become very important until the lowest temperatures.

C. Internal Energy and Enthalpy in Applied Fields

In the presence of an applied magnetic field there is some ambiguity in the definitions of energy U and enthalpy E, depending on whether one includes the energy associated with the field outside the sample or not.[88] In this paper we shall choose the definitions implied by

$$dU = TdS + HdM \tag{10}$$

and

$$dE = TdS - MdH, \tag{11}$$

since these correspond most directly with the usual gas forms, with H corresponding to $-p$ and M to V. Using the thermal and magnetic data already presented we can readily obtain changes in U and E between any two temperatures at constant field H_0 by simply integrating C_{H_0}:

$$\begin{aligned}(\Delta U)_{H_0} &= \int_{T_1}^{T_2} C_{H_0}\,dT + H_0(M_2 - M_1),\\ (\Delta E)_{H_0} &= \int_{T_1}^{T_2} C_{H_0}\,dT,\end{aligned} \tag{12}$$

where M_1 and M_2 are the corresponding magnetic moments. To relate the curves for different fields we can use the isothermal changes in S and M at some arbitrary temperature T',

$$\begin{aligned}(\Delta U)_{T'} &= T'(S_{H_0} - S_{H_0=0}) + \int_0^{H_0} H_0\,dM_{T'}\,,\\ (\Delta E)_{T'} &= T'(S_{H_0} - S_{H_0=0}) - \int_0^{H_0} M_{T'}\,dH_0,\end{aligned} \tag{13}$$

relative to the zero field $U-T$ curve already established. (In zero field, $U_{H_0=0}$ and $E_{H_0=0}$ are identical.) The results are shown in Figs. 22 and 24. If we had used the alternative definitions of U and E (the so-called spectroscopic energies commonly used in statistical mechanics calculations), these two sets of curves would have been interchanged. In Fig. 25 we show a plot of E as a function of S for various fixed H_0 and T, which is the magnetic analog of the Mollier chart commonly used in thermodynamic calculations.[89,90]

It can be seen from Fig. 22 that the internal energy in high fields becomes very small and nearly independent of H_0 as T tends to zero, in agreement with our earlier conclusion that the interactions tend to cancel in the aligned paramagnetic state. The low-field curves likewise tend to a common value, corresponding to the fact that the antiferromagnetic state of a highly anisotropic system is practically unaffected by a weak field ($H_0 < H_0^-$) as $T \to 0\,^{\circ}\mathrm{K}$.

The corresponding curves for the enthalpy are perhaps more obvious intuitively, since we might expect the appropriate energy to tend to $-MH_0$ if the interactions tend really to cancel the paramagnetic state. For the highest field shown, $H_0 = 10.16$

kOe and $M = M_0 = 666$ emu/cm^3; this corresponds to $E_0/R = -3.54$, in good agreement with -3.5 ± 0.1 indicated by the curve in Fig. 24. In order to make more detailed and precise comparisons of this sort, we would really need additional data at lower temperatures, but these are not available at this time.

However, the present curves may also be used in another way to make more general, purely thermodynamic predictions of temperature and heat changes corresponding to changes in the applied field. These would be of interest in the design of possible heat engines using DAG as the working medium.

D. Magnetic Heat Engines

The complete analogy between the thermodynamic properties of a system like DAG with those of a more usual liquid-gas system suggests that it might be interesting to consider the corresponding analogs of some of the applications to heat engines. Such a device might perhaps be useful for maintaining a temperature below 4.2 °K without the necessity of large vacuum pumps, and if the field were supplied by a permanent magnet, it would only dissipate energy through the evaporation of liquid helium at 4.2 °K and the performance of an insignificant amount of mechanical work in moving the sample relative to the field.

To obtain an estimate of the amounts of heat which could be handled by such a device, it is easiest to look at the S-T diagram on which a Carnot cycle is a simple rectangle. For example, from Fig. 21 one can see that starting at 4.2 °K and 14 kOe one can reach 2.0 °K by demagnetizing adiabatically to a field of 3 kOe. If thermal contact were established with a heat source at this temperature and the field increased to 5 kOe, an amount of heat

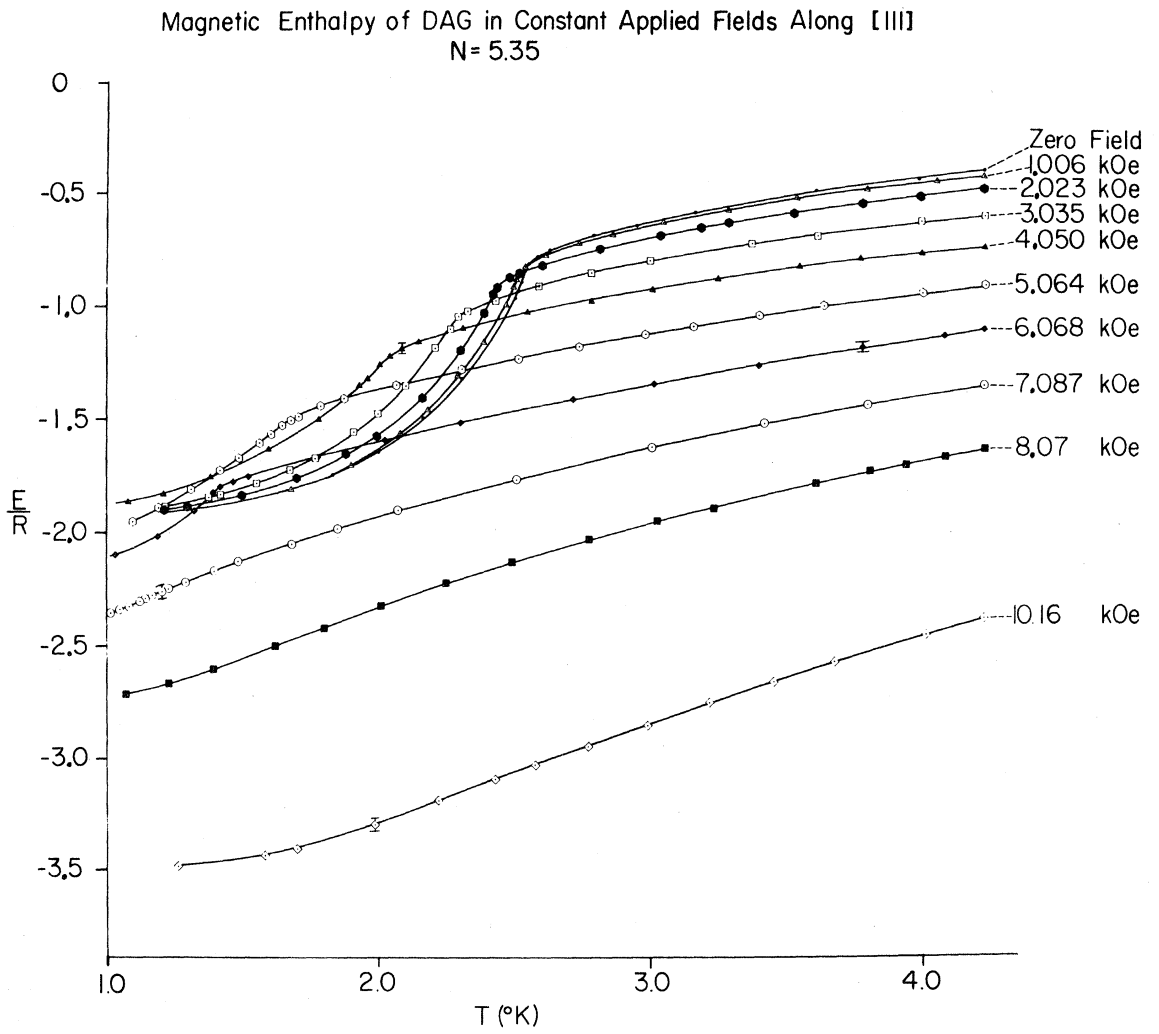

FIG. 24. Magnetic enthalpy E/R of DAG as a function of temperature in constant applied magnetic fields H_0 along [111] for $N = 5.35$. The zero is the same as that of U/R (which is equal to E/R for $H = 0$.)

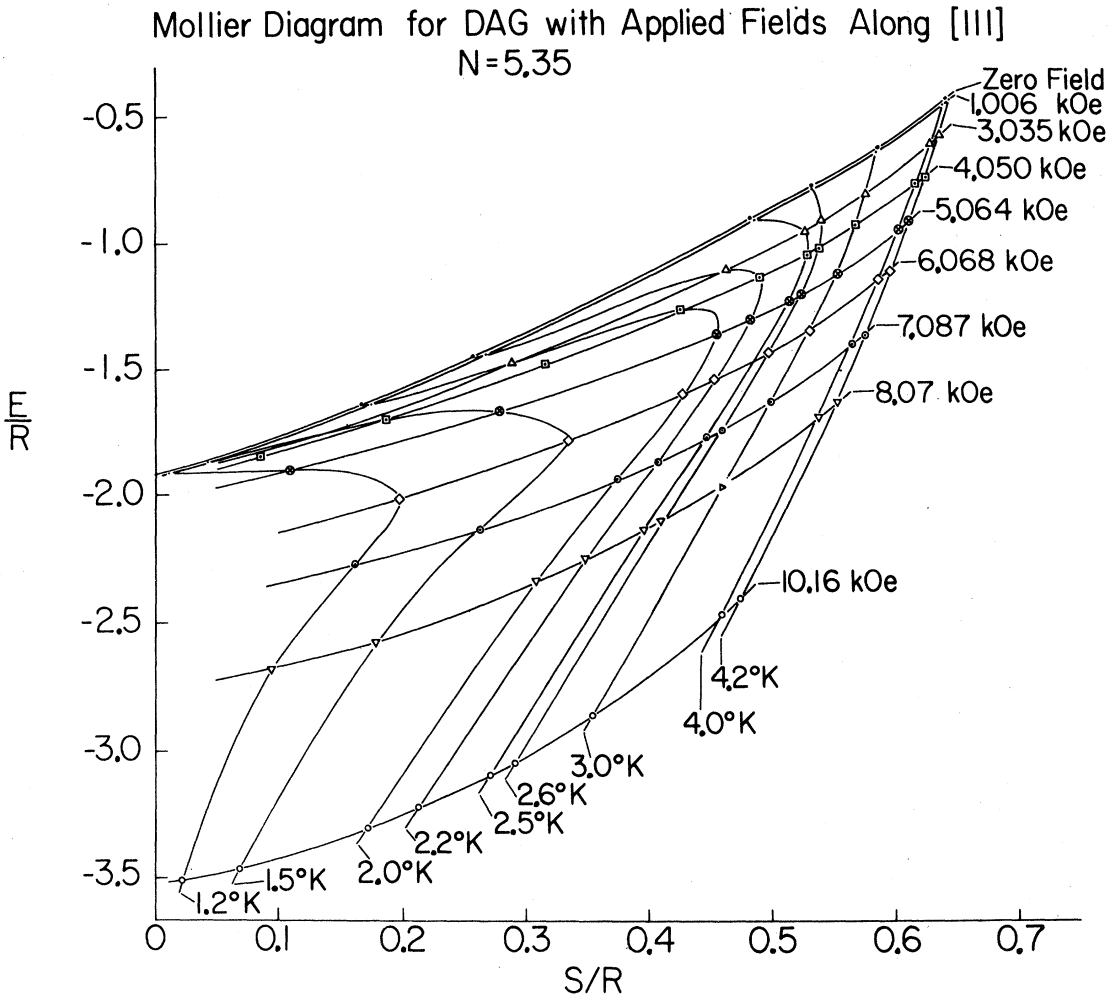

FIG. 25. Enthalpy as a function of entropy (Mollier diagram) for DAG showing lines of constant temperature and constant applied field H_0 along [111], appropriate to a sample with $N=5.35$.

given by $T\Delta S = 0.3R$ could be extracted for useful cooling. To complete the cycle one would magnetize adiabatically to a field of 10 kOe which should bring the temperature back to 4.2 °K where further magnetization to 14 kOe in thermal contact with the helium bath would restore the initial conditions. Expressed in practical units, this example shows that 1 mole of DAG (about 43 cm^3 in volume) could extract 2.4 J/cycle at a temperature of 2.0 °K. If we estimate, perhaps overoptimistically, a cycle time of 1 min this corresponds to a cooling power of 0.06 W which would be equivalent to an evaporation of liquid helium of about 80 cm^3/h, a fairly typical rate for a laboratory cryostat.

While this example shows that the heat extraction rate is reasonable, it is not really clear that such a device would offer any significant advantages for most applications. However, it may be capable of development and in particular it may prove possible to use the one additional property in which a magnetic material differs from gas-liquid system: the anisotropy with respect to the direction of the applied magnetic field. So far in this paper we have only considered fields applied along [111], but it is clear from the general nature of DAG that measurements in other directions will yield significantly different properties. Some of these will be discussed in III[91] and we note here only that significant cooling has in fact been observed in adiabatic rotation experiments in fixed fields (e.g., 1.8 – 0.55 °K in 12 kOe). This suggests that one might be able to make a useful refrigerator for very much lower temperatures than those discussed above, either by using this effect directly or else by performing Carnot-type cycles with fields in other directions. We shall return to these ideas in paper III.

VI. SHAPE DEPENDENCE OF THERMODYNAMIC FUNCTIONS

So far we have considered the thermal properties only as functions of T and the *applied* magnetic field H_0, but in terms of these variables the prop-

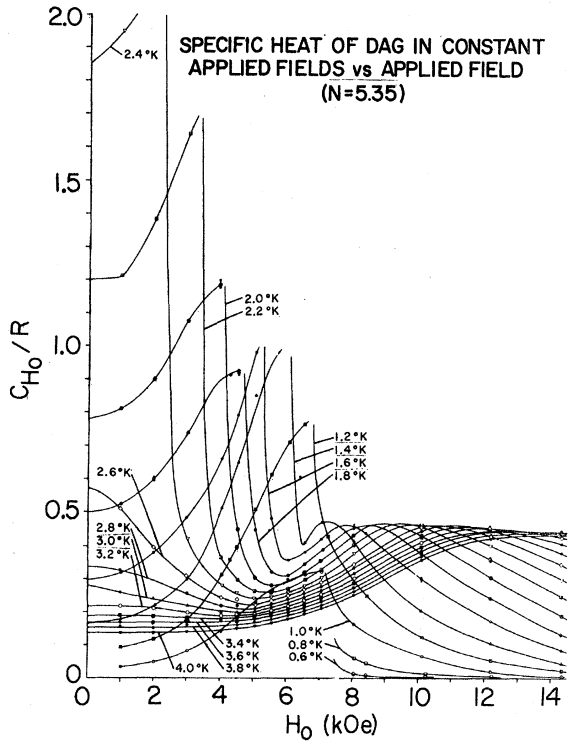

FIG. 26. Specific heat of DAG at constant applied field, C_{H_0}/R, as a function of applied field, H_0 along [111], for a sample with $N=5.35$. From these curves one can find C_{H_0}/R as a function of the internal field and temperature which may then be used to derive $C_{H_i}(H_i, T)$ by means of Eq. (17).

erties will depend on sample shape and our results are only valid for the particular case of $N=5.35$. To relate the properties to other sample shapes it is convenient to express all functions in terms of H_i, the internal field defined in Eq. (3), and in principle this can always be done, provided the sample is a homogenous ellipsoid.

In practice this turns out to be considerably more difficult than the corresponding transformation for the magnetic properties (see Sec. III). One reason for this lies in the fact that measurements made in constant external fields correspond to different *varying* internal fields as T is changed, and in order to construct a plot at *constant* internal field, results from many experimental curves must be combined. In practice one is frequently forced to interpolate and this is particularly serious near phase transitions, where functions vary rapidly.

Another difficulty lies in the fact that the relationship between H_0 and H_i involves M, so that the transformation of purely thermal properties also entails a knowledge of the magnetic properties at the same point. This again forces one to interpolate, but even worse, one must generally use data obtained on a different sample in a different apparatus and small systematic differences can easily occur. These are again most serious near phase transitions which are unfortunately the regions of greatest interest theoretically.

For the present we shall try to remove the shape effects as best we can but with a warning that some of the critical behavior may be subject to relatively large errors due to the factors discussed above.

In Sec. VIA we shall derive specifically curves of C_{H_i} and S as a function of T for various fixed H_i. Curves for U and E at constant H_i have not been constructed, but specific values could be worked out fairly easily using Eq. (3′) and Fig. 2 in conjunction with Figs. 22 and 24. The corresponding free energies $U-TS$ and $E-TS$ could likewise be computed from the data given but we have not done this either as there is no immediate need for these curves.

A. Derivation of $C_{H_i}(T,H_i)$

The derivation of C_{H_i} from C_{H_0} has been discussed by Levy and Landau.[42,92] The simplest approach is a purely thermodynamic one, in which one calculates the change of entropy for small change in T, keeping H_0 constant. In such a process the internal field changes by a small amount ΔH_i which is given by

$$\Delta H_i = -N\Delta M = -N\left(\frac{\partial M}{\partial T}\right)_{H_0}\Delta T\,, \tag{14}$$

and the change of entropy is thus the sum of two terms

$$\Delta S=\left(\frac{\partial S}{\partial T}\right)_{H_i}\Delta T+\left(\frac{\partial S}{\partial H_i}\right)_T\Delta H_i$$

$$=\left[\left(\frac{\partial S}{\partial T}\right)_{H_i}-N\left(\frac{\partial S}{\partial H_i}\right)_T\left(\frac{\partial M}{\partial T}\right)_{H_0}\right]\Delta T\,. \tag{15}$$

Using standard identities this can be written as

$$C_{H_0}=C_{H_i}-N\left(\frac{\partial M}{\partial T}\right)_{H_i}\left(\frac{\partial M}{\partial T}\right)_{H_0}\,. \tag{16}$$

Eliminating the term involving H_0 in a similar way, one finds finally

$$C_{H_i}=C_{H_0}+T\left(\frac{\partial M}{\partial T}\right)^2_{H_i}\Big/\left[\frac{1}{N}+\left(\frac{\partial M}{\partial H_i}\right)_T\right]\,. \tag{17}$$

To determine C_{H_i} as a function of T and H_i from the experimental data one must therefore first express C_{H_0} as a function of T and H_i. This involves plotting C_{H_0} as a function of H_0 at fixed T, as shown in Fig. 26, and reading off values for fields corresponding to given values of H_i. For this one requires a relationship between H_0 and H_i which can be found using Eq. (3) and the magnetic isotherms of Fig. 5.

The second term in Eq. (17) involves two derivatives which have already been given in Figs. 7

and 10 and in principle the evaluation of this term should present no difficulty. In practice, however, the contribution from this term can be very large and it is necessary to estimate the derivatives with care. Since both are large and rapidly varying close to the phase boundary, additional measurements of $M(H_0, T)$ were therefore made in this general region at a number of closely spaced temperatures (0.025 °K) and fields (25 Oe), and these were used to improve the accuracy of Figs. 7 and 10. Using these derivatives together with $C_{H_0}(T, H_i)$ we finally obtain $C_{H_i}(T, H_i)$ as shown in Fig. 27.

The results are quite striking when compared with the curves of C_{H_0} vs T shown in Figs. 15–17. The "corrected" specific heats are clearly much sharper and higher, and one might speculate that they could be intrinsically infinite. However, even though the over-all temperature resolution of the present data is not very high, it seems quite clear that all the peaks above 1.66 °K are in fact definitely *finite*, since there is no evidence that $(\partial M/\partial T)_{H_i}$ diverges (see Figs. 9 and 10), and C_{H_0} certainly remains finite throughout (see Figs. 15–17). We thus conclude that $(\partial M/\partial T)_{H_i}$ and C_{H_i}

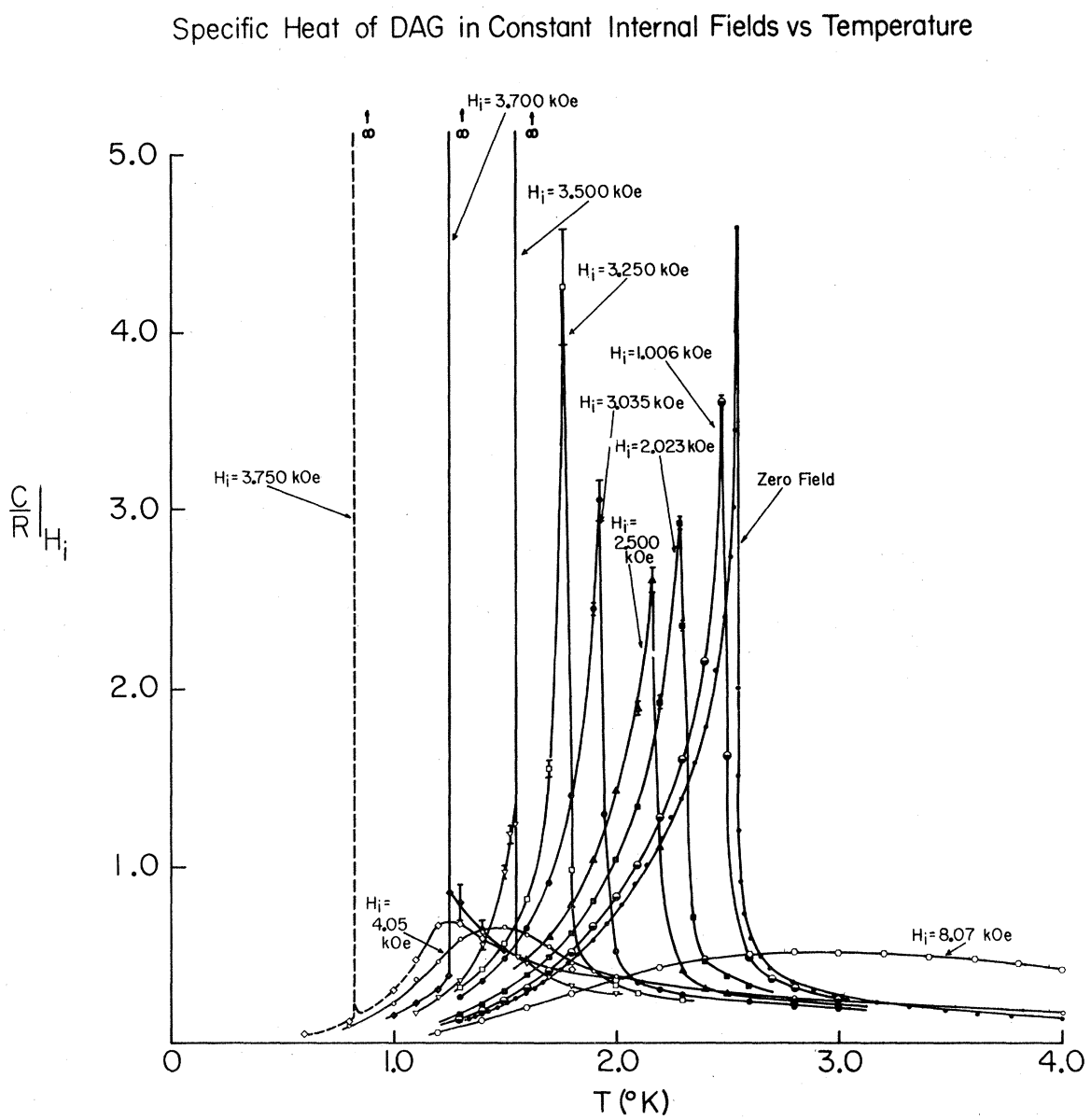

FIG. 27. Specific heat of DAG at constant internal field C_{H_i} as a function of temperature for different internal fields H_i along [111], calculated from measurements on samples with $N = 5.35$ and 4.19 using Eq. (17). In principle these curves could also be measured directly on a long thin sample for which $H_i \approx H_0$. The δ-function peaks appearing below 1.66 °K correspond to the latent heat which accompanies the first-order transition in constant H_i (see Fig. 20).

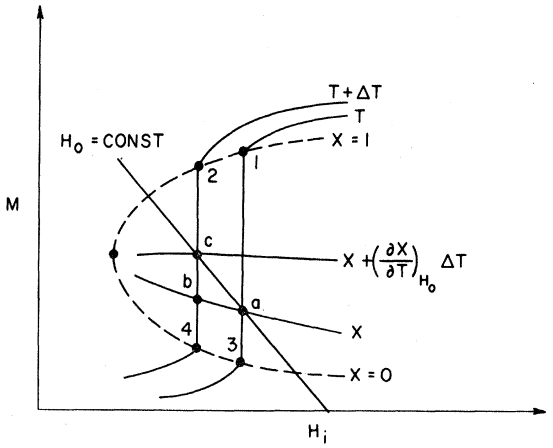

FIG. 28. Schematic phase diagram in the M-H_i plane showing two adjacent isotherms for $T < T_t$ (i.e., in the first-order region). The line $H_0 = \text{const}$ defines $H_i = H_0 - NM$, and it shows how heating at constant H_0 corresponds to a change in H_i. The lines of constant x represent constant fractions of the antiferromagnetic and paramagnetic phases which coexist inside the first-order transition region.

as well as $(\partial M/\partial H_i)_T$ all remain finite for $T_t < T < T_N$, consistent with our earlier identification of the phase transition as one of "higher order" (i.e., neither first order nor the usual λ type of second-order transition).

Below T_t the latent heat now appears as a δ function in C_{H_i} and it is quite difficult to determine the variation of C_{H_i} as T approaches the first-order transition. It would seem that C_{H_i} is also finite in this region but additional measurements are really required to clarify this question.

B. Estimates of C_{H+} and C_{H-}

In addition to specific heats at constant fields, we can define two other specific heats, which in a liquid-gas system would correspond to the heat capacities of the saturated vapor and liquid *along* the phase boundary. In Fig. 28 we show schematically two adjacent isotherms and the phase boundary in the M-H_i plane, and we see that we can define a specific heat along the upper (paramagnetic) phase boundary, $C_{H+} = T(S_2 - S_1)/\Delta T$, where 1 and 2 refer to points on the first-order line at temperatures T and $T+\Delta T$. Likewise we define the specific heat along the lower (antiferromagnetic) phase boundary $C_{H-} = T(S_4 - S_3)/\Delta T$.

C_{H+} and C_{H-} can be derived from the data already presented, using an analysis similar to that used to relate C_{H_0} to C_{H_i}. When the system is in the mixed antiferromagnetic-paramagnetic state, at a point such as a in Fig. 28, a small change of T at constant H_0 produces a rather complex change of state which can be resolved into two parts. If x is the fraction of paramagnetic phase present, then the thermal change along $a-b$, keeping x constant, corresponds simply to the weighted heat capacity $C_{H+} + (1-x)C_{H-}$. But if the measurements are made keeping H_0 constant x will in fact change by an amount $(\partial x/\partial T)\Delta T$, and the thermal change along $b-c$ will then correspond to a partial transformation of antiferromagnetic phase into paramagnetic phase. This will involve an additional amount of latent heat given by $L(\partial x/\partial T)_{H_0}\Delta T$. We can thus write

$$C_{H_0}(H_0, T) = xC_{H+} + (1-x)C_{H-} + L\left(\frac{\partial x}{\partial T}\right)_{H_0} \tag{18}$$

for any point (H_0, T) in the mixed phase.

The quantity x, which is known as the "quality factor" in the case of steam,[89] can be determined from the magnetic isotherms and plotted as a function of T for different fields H_0 to find $(\partial x/\partial T)_{H_0}$. The latent heat L can be taken from Fig. 20 and one can thus plot $C_{H_0} - L(\partial x/\partial T)_{H_0}$ as a function of x to determine C_{H+} and C_{H-}. The results are shown in Fig. 29.

The errors in these determinations are clearly quite large, but it is apparent that C_{H+} and C_{H-} vary quite differently with temperature. The difference between the two curves can be checked thermodynamically by noting that $C_{H+} - C_{H-} = dL/dT$, and in particular we can check that the crossing at 1.43 °K corresponds to the observed maximum in L. But

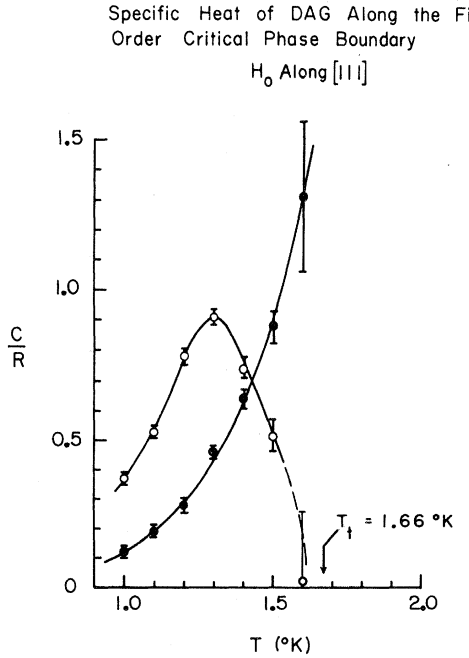

FIG. 29. Specific heats of DAG *along* the first-order phase boundary. Closed circles are the specific heat C_{H-} along the lower (antiferromagnetic) phase boundary (3→4 in Fig. 28); open circles are the specific heat C_{H+} along the upper (paramagnetic) phase boundary (1→2 in Fig. 28).

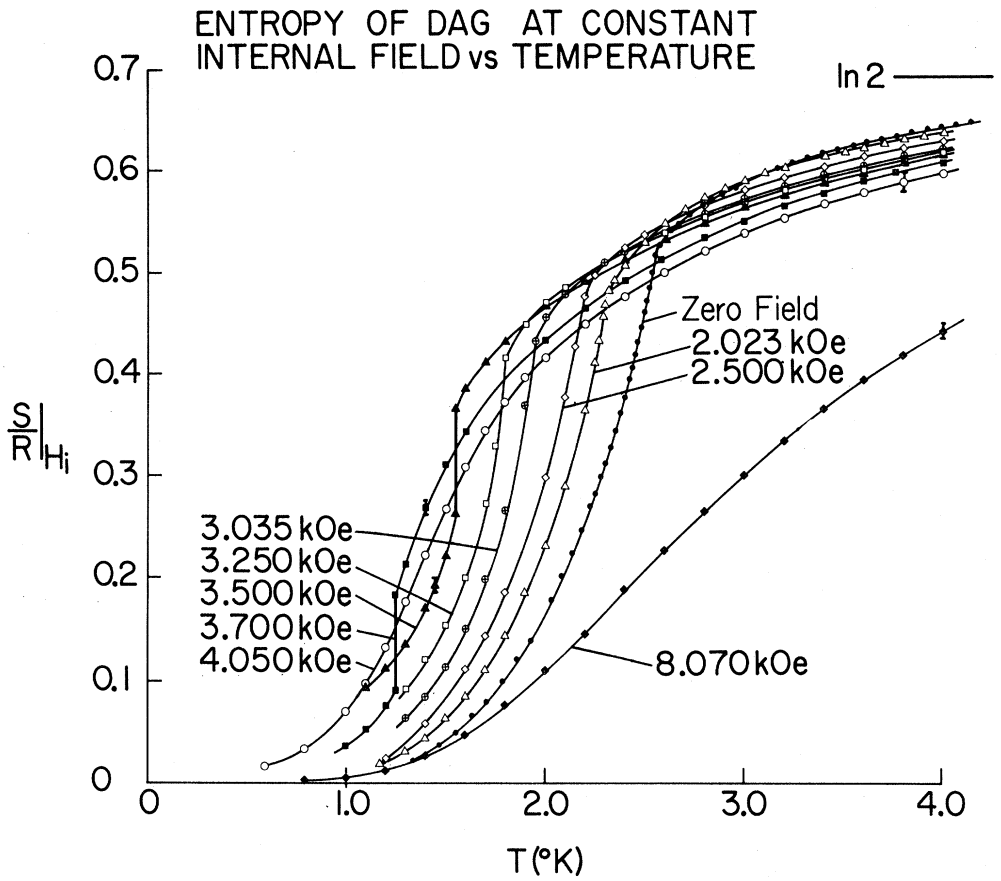

FIG. 30. Entropy of DAG as a function of temperature for constant internal fields H_i along [111]. The discontinuities on the curve for $H=3.5$ and 3.7 kOe correspond to the latent heat associated with the first-order phase change.

there is no microscopic theory for the temperature variation of any of these quantities and we can only speculate on the strength of the present results that C_{H-} might in fact diverge while C_{H+} becomes small or even negative as T approaches $T_t = 1.66$ °K. Further experiments specifically designed to measure C_{H+} and C_{H-}, as well as a theoretical study of the whole first-order phase transition, would clearly be of interest.

C. Determination of $S(T,H_i)$

The variation of entropy with temperature at constant *internal* field can be derived from the data in two ways. One way is to start from the curves of S vs T and constant *applied* fields already given in Fig. 21. Interpolating can then find $S(T, H_0)$ for different values of H_0 and in particular for values of H_0 corresponding to given values of H_i calculated from Eq. (3′) and the magnetization data in Fig. 2. An alternative method is to integrate the C_{H_i} vs T at constant H_i curves given in Fig. 27 using Eq. (7a), as in the case of constant applied fields (see Sec. V). The difficulty is again the problem of estimating the high- and low-temperature extrapolations, though these will be quite similar to the extrapolations at constant H_0. There is also a minor difficulty in the regions of the first-order transition where C_{H_i} simply shows a δ function which can not be integrated directly. However, the corresponding change of entropy is obtained easily from the latent heat curve in Fig. 20 using $\Delta S = L/T$.

Combining both methods one obtains the results shown in Fig. 30. These curves are generally similar to those for constant H_0, except that the change from higher order to first is now clearly apparent.

The consistency of these results was checked as for the M-T-H_i surface, by estimating orthogonal derivatives at selected points on the S-T-H_i surface and evaluating the product $(\partial S/\partial T)_{H_i}(\partial T/\partial H_i)_S \times(\partial H_i/\partial S)_T$. Values ranging from -0.89 to -1.27 were found, but in all cases the estimated error limits covered the ideal value, -1.

VII. CONCLUSIONS

In this paper we have presented the results of a rather detailed series of thermal and magnetic measurements on single crystals of DAG with magnetic fields applied in the symmetry direction [111]. For this orientation DAG behaves like a two-sublattice

Ising antiferromagnet and one can study the antiferromagnetic-paramagnetic phase transition as a function of field and temperature. One factor which simplifies this study is the fact that the magnetic interactions are very much weaker than the lattice energies ($T_N/\Theta_D \sim 2.5/500$) and not particularly strain sensitive, so that the system can be treated as purely magnetic, without any complications from elastic or magnetoelastic effects. The experimentally obtained quantities can therefore be used to construct a complete thermodynamic picture in terms of the variables M, H, T, in direct analogy with the corresponding functions of V, p, T for a liquid-gas system.

A magnetic phase diagram has been constructed, and this reveals a number of features not commonly found for other magnetic systems nor for the liquid-gas case. In zero field there is typical "second-order" transition, with a sharp but slightly rounded λ anomaly in the specific heat as usual, but the similarity of the results observed for four different samples suggests that the observed rounding might perhaps be an intrinsic property in DAG and not the result of impurities as is generally assumed. In finite fields the properties become dependent on the sample shape, as one would expect, but even if this effect is "removed" by expressing all the results in terms of internal magnetic fields, the behavior is quite unusual.

For small internal fields, the transitions are marked by sharp but definitely *finite* peaks in $(\partial M/\partial H_i)_T$, $(\partial M/\partial T)_{H_i}$, and C_{H_i} which respectively correspond to $\partial^2 F/\partial M_i^2$, $\partial^2 F/\partial H_i \partial T$, and $T(\partial^2 F/\partial T^2)$. The lack of either infinite singularities or discontinuities in these quantities[93] seems to rule out the possibility that the phase transition in the presence of a field is of the usual second-order type and we are forced to conclude that it must be a more diffuse "higher-order" type.[64] This in turn would seem to imply that the transition in zero field is either intrinsically different in character from the transition in a field or else also of "higher order." Neither of these two possibilities would correspond to current statistical theories of antiferromagnetic phase transitions, which all assume a *similar* and generally singular behavior *with and without* an applied field.

As the field is increased the character of the transition changes quite gradually, appearing to get sharper until it becomes clearly of first order at the point ($T_t = 1.66\,^\circ$K, $M_t = 250$ emu/cm^3, $H_i^t = 3.25$ kOe). The first-order transition is accompanied by a latent heat which has been measured and compared with the thermodynamic predictions of the Clausius-Clapeyron equation. Good agreement was found. The first-order transition also implies a phase separation involving the coexistence of regions of the antiferromagnetic and paramagnetic phases, but the phase separation is unusual in that there is evidence that the phases are so intimately mixed that the system can still be treated as effectively homogeneous with respect to its thermodynamic properties.

Apart from the nature of the mixed phase, the whole behavior is clearly reminiscent of the phase diagram for He^3-He^4 mixtures, as discussed recently by Griffiths.[58] Although it is not obvious that the two cases must correspond in detail, it may well turn out that DAG will serve as a useful model for further theoretical study of this type of system, since the correspondence with a regular lattice-gas Ising model is clearly more direct than in the case of a liquid. The present paper is restricted to a discussion in terms of classical thermodynamics, and we defer until a later paper in the series a more detailed analysis in terms of a microscopic Hamiltonian. However, it is interesting to speculate already at this stage what general feature of the interactions might be responsible for the unusual phase transitions observed in DAG. We can identify two potentially important factors which are both related to the long-range character of the magnetic dipole interactions known to be dominant in DAG.[6,94]

One result of this is a competition between the interactions coupling different *near* neighbors, so that some favor the paramagnetic state, while others favor the antiferromagnetic state. The second is a cumulative contribution to the energy from the interaction with many *distant* neighbors, which in general depends on the shape of the sample but vanishes when $M = 0$. One therefore again has a competition between forces favoring different magnetic states.

The only theoretical model available at this time is the mean field approximation[95–97] which does not differentiate between these two factors, and it seems clear that further study is called for. However, even in the absence of a microscopic theory we can draw some interesting conclusions from the experimental results themselves. It was found that the intrinsic first-order transition only becomes apparent when the results are expressed in terms of the internal field, corresponding to a long thin sample, and one might conclude that this is equivalent to removing the long-range dipolar effects. In fact, however, this procedure *maximizes* the dipolar contribution by merely removing the negative demagnetizing field due to the free surface, and we can conclude therefore that the long-range dipolar field in the magnetized state is indeed one important factor for the first-order transition in DAG. Since the dipolar field is largest for a long needle, any finite sample would then always break up into thin domains,[60] and the intrinsic properties would be those of such a domain.

It would appear therefore that any theoretical model which is restricted to only near neighbors could not hope to reproduce the observed behavior, and it would seem essential to consider models in which long-range interactions are included explicitly. However, it is still possible that the first-order transition may *also* result from competing near-neighbor interactions, and that the long-range dipolar field merely lowers the energy at the phase transition. If this in fact turns out to be the case, we might expect the similarity between DAG and He^3-He^4 mixtures to be more than just accidental, since there can be little doubt that the He^3-He^4 system is dominated by competing short-range forces. On the other hand, if the long-range forces in DAG turn out to be primarily responsible for the phase transition the similarity may be just superficial.

A clarification of these questions must await further theoretical developments. But before a realistic model for DAG can in fact be constructed, it will be necessary to obtain explicit estimates of the strength of different interactions and the values of the relevant dipolar lattice sums. This we shall do in further papers in the present series.

ACKNOWLEDGMENTS

We would like to thank M. Blume, M. E. Fisher, R. B. Griffiths, P. M. Levy, H. Wagner, and A. F. G. Wyatt for a number of helpful discussions and we would also like to thank C. A. Catanese for assistance with some of the experiments. The two cryostats used for these experiments were constructed by C. Sneider and we are pleased to acknowledge his skillful work. One of us (W. P. W) would like to express his appreciation to the Physics Department of the Brookhaven National Laboratory for their gracious hospitality during the preparation of the final manuscript.

APPENDIX: SPECIFIC HEATS OF YAG AND LuAG

Yttrium aluminum garnet (YAG) and Lutetium aluminum garnet (LuAG) are both diamagnetic and isostructural with DAG, and their specific heats should provide a good basis for estimating the lattice contribution to the thermal properties of DAG.

Polycrystalline samples of both garnets were made by the standard coprecipitation method,[98] compressed into cylinders about 20 g in weight, and fired at 1400 °C for 24 h to ensure a complete reaction. X-ray diffraction showed no trace of any phase other than garnet. The samples were held in a brass holder and supported by cotton threads, as for the zero-field DAG measurements, using N grease to ensure thermal contact. Heat-capacity measurements were made on both samples and the empty holder up to about 6 °K, above which the experimental scatter became rather large.

The results for all runs obeyed the expected form[99]

$$C/R = \gamma T + AT^3 , \tag{A1}$$

where the first term is the electronic contribution from the brass, and the second term is the lattice contribution from the garnet and/or the holder and thermometer. Subtracting, one can thus find A (YAG) and A (LuAG). In practice, the heat capacity of the holder was found to be about five times larger than that of the garnet samples with both very small, and this results in a rather large error in the A's. Moreover, since the lattice specific heat is so small the measurement is quite susceptible to error from magnetic impurities, although we would not expect this contribution to be particularly large for the samples used. For the present purpose all these uncertainties are not very serious, and we finally estimate

$$A(\mathrm{YAG}) = (0.87 \pm 0.10) \times 10^{-5} ,$$

$$A(\mathrm{LuAG}) = (1.10 \pm 0.12) \times 10^{-5} .$$

The corresponding Debye Θ's assuming that only the rare-earth ions contribute are given by[100]

$$\Theta_D(\mathrm{YAG}) = (545 \pm 20)\ ^\circ\mathrm{K}$$

and

$$\Theta_D(\mathrm{LuAG}) = (500 \pm 20)\ ^\circ\mathrm{K} .$$

The difference between the YAG and LuAG results is, of course, not unexpected, since there is a considerable difference in the atomic masses of Y and Lu (89 and 175, respectively). If we make the simplest approximation and attempt to scale the Θ_D's using the Debye relation[101] $\Theta_D \propto m^{-1/2}$, we would predict $\Theta_D(\mathrm{DAG}) = 465\ ^\circ\mathrm{K}$ from the YAG results and $\Theta_D(\mathrm{DAG}) = 511\ ^\circ\mathrm{K}$ from the LuAG results. The agreement is about as good as one would expect in view of the crudeness of the extrapolation, and it seems clear that one should place more weight on the value obtained from the LuAG measurements for which the extrapolation is much smaller. We finally estimate, therefore,

$$\Theta_D(\mathrm{DAG}) = (500 \pm 30)\ ^\circ\mathrm{K},$$

which is equivalent to

$$(C/R)_{\mathrm{lattice}} = (1.1 \pm 0.2) \times 10^{-5} T^3 .$$

Although the measurements were made only up to 6 °K this result is probably valid up to at least 10 °K, since the T^3 law is generally applicable to about $\Theta_D/50$. In any case, the lattice specific heat will be less than $10^{-2}R$ over the entire range of the magnetic measurements, and near T_N it will be less than $2 \times 10^{-4}R$. In this region the lattice contribution is thus entirely negligible and only at the highest temperatures is a small correction necessary.

*Work supported in part by the U. S. Atomic Energy Commission.

†Present address: Department of Physics, University of Georgia, Athens, Ga. 30601.

‡Present address: United Kingdom Atomic Energy Authority, Culham Laboratory, Culham, Abingdon, Berks, England.

§Present address: Philips Research Laboratory, Hamburg, Germany.

[1]M. Ball, M. T. Hutchings, M. J. M. Leask, and W. P. Wolf, in *Proceedings of Eighth International Conference on Low Temperature Physics*, edited by R. A. Davis (Butterworths, London, England, 1963), p. 248.

[2]A. F. G. Wyatt, thesis, Oxford University, 1963 (unpublished).

[3]W. P. Wolf, in *Proceedings of the International Conference on Magnetism, Nottingham, England*, 1964 (The Institute of Physics and The Physical Society, London, England, 1964), p. 555.

[4]M. Ball, W. P. Wolf, and A. F. G. Wyatt, Phys. Letters 10, 7 (1964).

[5]R. Bidaux, P. Carrara, and B. Vivet, J. Phys. (Paris) 29, 357 (1968).

[6]M. Ball, M. J. M. Leask, W. P. Wolf, and A. F. G. Wyatt, J. Appl. Phys. 34, 1104 (1963).

[7]B. E. Keen, D. Landau, B. Schneider, and W. P. Wolf, J. Appl. Phys. 37, 1120 (1966).

[8]D. P. Landau, thesis, Yale University, 1967 (unpublished).

[9]B. E. Keen, D. P. Landau, and W. P. Wolf, Phys. Letters 23, 202 (1966).

[10]B. E. Keen, D. P. Landau, and W. P. Wolf, J. Appl. Phys. 38, 967 (1967).

[11]W. P. Wolf, B. E. Keen, D. P. Landau, and B. Schneider, in *Proceedings of the Tenth International Conference on Low Temperature Physics, Moscow*, 1966, edited by M. P. Malkov (Vimiti Publishing House, Moscow, 1967), Vol. 4, p. 136.

[12]W. P. Wolf, M. Ball, M. T. Hutchings, M. J. M. Leask, and A. F. G. Wyatt, J. Phys. Soc. Japan Suppl. 17, 443 (1962).

[13]I. Svare and G. Seidel, in *Paramagnetic Resonance*, edited by W. Low (Academic, New York, 1963), p. 430.

[14]A. J. Lindop, thesis, Oxford University, 1966 (unpublished).

[15]D. T. Edmonds and A. J. Lindop, J. Appl. Phys. 39, 1108 (1968).

[16]F. Bertaut and F. Forrat, Compt. Rend. Acad. Sci. 244 (1957).

[17]A. Herpin and P. Mériel, Compt. Rend. 259, 2416 (1964).

[18]J. M. Hastings, L. M. Corliss, and C. G. Windsor, Phys. Rev. 138, A176 (1965).

[19]J. C. Norvell, L. M. Corliss, J. M. Hastings, R. Nathans, and W. P. Wolf, J. Appl. Phys. 39, 1232 (1968).

[20]J. C. Norvell, thesis, Yale University, 1968 (unpublished).

[21]J. C. Norvell, W. P. Wolf, L. M. Corliss, J. M. Hastings, and R. Nathans, Phys. Rev. 186, 557 (1969).

[22]J. C. Norvell, W. P. Wolf, L. M. Corliss, J. M. Hastings, and R. Nathans, Phys. Rev. 186, 567 (1969).

[23]K. H. Hellwege, S. Hüfner, M. Schinkman, and H. Schmidt, Phys. Letters 12, 107 (1964).

[24]A. H. Cooke, K. A. Gehring, M. J. M. Leask, D. Smith, and J. H. M. Thornley, Phys. Rev. Letters 14, 685 (1965).

[25]S. Hüfner, M. Schinkman, and H. Schmidt, Physik Kondensierten Materie 4, 108 (1965).

[26]K. A. Gehring, M. J. M. Leask, and J. H. M. Thornley, Czech. J. Phys. 17, 369 (1967).

[27]P. Grünberg, K. H. Hellwege, and S. Hüfner, Physik Kondensierten Materie 6, 95 (1967).

[28]R. C. Milward, Phys. Letters 25A, 19 (1967).

[29]M. J. M. Leask, J. Appl. Phys. 39, 908 (1968).

[30]P. Grünberg, S. Hüfner, E. Orlich, and J. Schmitt, J. Appl. Phys. 40, 1501 (1969).

[31]K. Aoyagi, K. Tsushima, and M. Uesugi, J. Phys. Soc. Japan 27, 49 (1969).

[32]S. Washimiya, J. Phys. Soc. Japan 27, 56 (1969).

[33]K. A. Gehring, M. J. M. Leask, and J. H. M. Thornley, J. Phys. C 2, 484 (1969).

[34]R. Faulhaber and S. Hüfner, Z. Physik 228, 235 (1969).

[35]R. Faulhaber and S. Hüfner, Solid State Commun. 7, 389 (1969).

[36]P. Grünberg, S. Hüfner, E. Orlich, and J. Schmitt, J. Appl. Phys. 40, 1501 (1969).

[37]P. Grünberg, S. Hüfner, E. Orlich, and J. Schmitt, Phys. Rev. 184, 285 (1969).

[38]I. Nowik and H. H. Wickman, Phys. Rev. 140, A869 (1965).

[39]J. I. Philp, R. Gonano, and E. D. Adams, J. Appl. Phys. 40, 1275 (1969).

[40]B. A. Calhoun and W. P. Wolf, Bull. Am. Phys. Soc. 11, 665 (1966).

[41]In an infinite cubic crystal there are, of course, eight equivalent ⟨111⟩ axes, but owing to demagnetizing effects the detailed behavior for fields applied along different ⟨111⟩ directions may be somewhat different in a finite crystal. To avoid the possibility of confusion, we shall only consider one particular ⟨111⟩ direction throughout and *define* this to be the [111] axis.

[42]P. M. Levy and D. P. Landau, J. Appl. Phys. 39, 1128 (1968).

[43]J. W. Nielsen, J. Appl. Phys. 31, 51S (1960).

[44]F. R. Charvet, J. C. Smith, and O. H. Nestor, J. Phys. Chem. Solids 45, (1967).

[45]S. Foner, Rev. Sci. Instr. 30, 548 (1969).

[46]R. M. Bozorth, *Ferromagnetism* (Van Nostrand, Princeton, N. J., 1951), p. 270.

[47]F. R. McKim and W. P. Wolf, J. Sci. Instr. 34, 64 (1957).

[48]G. Aubert, J. Appl. Phys. 39, 504 (1968).

[49]E. J. Walker, Rev. Sci. Instr. 30, 834 (1959).

[50]For rapid cooling in cases where later thermal isolation was not so important it was, of course, also possible to use exchange gas and for this purpose He^3 was used.

[51]J. E. Neighbor, Rev. Sci. Instr. 37, 497 (1966).

[52]A. C. Anderson, W. Reese, and J. C. Wheatley, Rev. Sci. Instr. 34, 1386 (1963).

[53]E. Ambler and H. Plumb, Rev. Sci. Instr. 31, 656 (1960).

[54]R. H. Sherman, S. G. Sydoriak, and T. R. Roberts, Report No. LAMS-2701, 1962 (unpublsihed).

[55]S. G. Sydoriak and T. R. Roberts, Phys. Rev. 102, 304 (1956).

[56]J. F. Cochran, C. A. Schiffman, and J. E. Neighbor, Rev. Sci. Instr. 37, 499 (1966).

[57]We wish to thank Dr. C. A. Schiffman for providing a specimen of pure lead.

[58]R. B. Griffiths, Phys. Rev. Letters 24, 715 (1970).

[59]An analysis of the available data indicates that M^+

$-M^-$ is approximately proportional to $(T_c - T)^{2/3}$, but as explained above, experimental difficulties preclude an accurate determination at this time. This will be discussed further in Paper II.

[60]A. F. G. Wyatt, J. Phys. C 1, 684 (1968).

[61]B. Schneider (unpublsihed).

[62]The same is not true in finite fields where spin-lattice effects are generally dominant and where the adiabatic and isothermal susceptibilities are different. For this reason it is not straightforward to extend ac measurements to nonzero applied fields and this explains why all the magnetization data reported in this paper were taken statically although ac techniques might have appeared attractive.

[63]It is found empirically that $(\partial M/\partial H_0)_T$ and $(\partial M/\partial H_i)_T$ peak at essentially the same value of H_0, implying that M at the inflection point is proportional to the corresponding H. Since the data are more closely spaced for H_0 it was most convenient to use $(\partial M/\partial H_0)_T$ to locate the phase transition.

[64]Boccara has pointed out (Ref. 65) that phase transitions such as the one described here may still be classified as "second order," if we include singularities in the antiferromagnetic order parameter. However, we prefer to describe the present transition as "higher order" to emphasize the fact that none of the *macroscopically* observable properties reveal any of the usual second-order behavior.

[65]N. Boccara, Solid State Commun. 7, 331 (1969).

[66]E. H. Graf, D. M. Lee, and J. D. Reppy, Phys. Rev. Letters 19, 417 (1967).

[67]See, for example, J. K. Roberts and A. R. Miller, *Heat and Thermodynamics* (Interscience, New York, 1960).

[68]We shall throughout express all thermal measurements in units of R, where $R = Nk_B$ and N is the number of magnetic ions. For a sample containing 1 g atom of magnetic ions $R = 8.317$ J/°K.

[69]M. E. Fisher, Phys. Rev. 176, 257 (1968).

[70]H. Wagner, Phys. Rev. Letters 25, 31 (1970).

[71]C. Domb and J. A. Wyles, J. Phys. C 2, 2435 (1969).

[72]The results over the whole range were also in general agreement with those reported earlier by Ball *et al.* (Ref. 6) except for a small shift in the peak temperature and also a small bump at 3.3 °K, which had been recognized as due to a perovskite impurity in the polycrystalline sample.

[73]D. T. Teaney, Phys. Rev. Letters 14, 898 (1965).

[74]P. Handler, D. E. Mapother, and M. Rayl, Phys. Rev. Letters 19, 356 (1967).

[75]C. S. Dixon and J. E. Rives, Phys. Rev. 177, 871 (1969).

[76]D. S. Gaunt and C. Domb, J. Phys. C 1, 1038 (1968).

[77]We are indebted to Professor H. Wagner for discussions of this possibility.

[78]Previous magnetothermodynamic studies on various other materials (see, for example, Refs. 79–85) have generally been somewhat limited by complications arising from weak and rather complex interactions, which lead to difficulties in both the experiments and their detailed analysis.

[79]C. B. G. Garrett, Proc. Roy. Soc. (London) A206, 242 (1951).

[80]J. H. Schelleng and S. A. Friedberg, Phys. Rev. 185, 728 (1969).

[81]N. J. Poulis and C. J. Gorter, in *Progress in Low Temperature Physics*, edited by C. J. Gorter (North-Holland, Amsterdam, 1955), p. 245.

[82]R. A. Fisher, E. W. Hornung, G. E. Brodale, and W. F. Giauque, J. Chem. Phys. 46, 4945 (1967).

[83]R. A. Fisher, G. E. Brodale, E. W. Hornung, and W. F. Giauque, J. Chem. Phys. 49, 4096 (1968).

[84]T. A. Reichert, R. A. Butera, and E. J. Schiller, Phys. Rev. B 1, 4446 (1970).

[85]J. E. Rives, Phys. Rev. 162, 491 (1967).

[86]In principle the term in b/T^2 should be subtracted from all measured specific heats to isolate the purely electronic parts, but in practice b is so small ($\sim 3\times10^{-3}$) that the contribution is negligible above about 1 °K.

[87]C. B. G. Garrett, *Magnetic Cooling* (Harvard U. P., Cambridge, Mass., 1954), p. 75.

[88]C. Kittel, *Elementary Statistical Physics* (Wiley, New York, 1958), p. 77.

[89]See, for example, M. Tribus, *Thermostatics and Thermodynamics* (Van Nostrand, New York, 1961), p. 276.

[90]It should be noted all these curves apply to a sample corresponding to $N = 5.35$. For other shapes there will be relatively small quantitative differences.

[91]See also Refs. 2 and 8.

[92]P. M. Levy, Phys. Rev. 170, 595 (1968).

[93]One can never rule out experimentally the possibility of a sufficiently small singularity in $(\partial M/\partial H_i)_T$, since one is always limited by finite resolution. However, in the present case we can place rather tight limits on any such singularity since points spaced by 25 Oe showed a perfectly smooth and continuous behavior at all temperatures, and it would therefore have to be limited to a region significantly smaller than this.

[94]B. Schneider, D. P. Landau, B. E. Keen, and W. P. Wolf, Phys. Letters 23, 210 (1966).

[95]C. B. G. Garrett, J. Chem. Phys. 19, 1154 (1951).

[96]K. Motizuki, J. Phys. Soc. Japan 14, 759 (1959).

[97]C. J. Gorter and T. Van Peski-Tinbergen, Physica 22, 273 (1956).

[98]W. P. Wolf and G. P. Rodrigue, J. Appl. Phys. 29, 105 (1958).

[99]Curves showing the actual results are given in Ref. 8.

[100]Using the relation $C = 234Nk_B\,(T/\Theta_D)^3$, where N is the number of heavy metal ions. If instead Θ_D is expressed in terms of one formula unit of $3R_2O_3 \cdot 5Al_2O_3$ (containing $6R^{3+}$ and 40 ions in all), our values of Θ_D must be multiplied by $(40/6)^{1/3} = 1.88$.

[101]M. Blackman, in *Handbuch der Physik*, edited by S. Flügge (Verlag, Berlin, 1955), Vol. 7, p. 325.